

# 1    Loss of ZnT8 function protects against diabetes by enhanced insulin 2    secretion

3

4    Om Prakash Dwivedi<sup>1#</sup>, Mikko Lehtovirta<sup>1#</sup>, Benoit Hastoy<sup>2#</sup>, Vikash Chandra<sup>3</sup>, Sandra Kleiner<sup>4</sup>,  
5    Deepak Jain<sup>5</sup>, Ann-Marie Richard<sup>6</sup>, Nicola L. Beer<sup>2</sup>, Nicole A. J. Krentz<sup>7</sup>, Rashmi B. Prasad<sup>8</sup>, Ola  
6    Hansson<sup>1,8</sup>, Emma Ahlqvist<sup>8</sup>, Ulrika Krus<sup>8</sup>, Isabella Artner<sup>8</sup>, Daniel Gomez<sup>4</sup>, Aris Baras<sup>4</sup>, Fernando  
7    Abaitua<sup>7</sup>, Benoite Champon<sup>7</sup>, Anthony J Payne<sup>7</sup>, Daniela Moralli<sup>7</sup>, Soren K. Thomsen<sup>2</sup>, Philipp  
8    Kramer<sup>7</sup>, Ioannis Spiliotis<sup>2</sup>, Reshma Ramracheya<sup>2</sup>, Pauline Chabosseau<sup>9</sup>, Andria Theodoulou<sup>9</sup>,  
9    Rebecca Cheung<sup>9</sup>, Martijn van de Bunt<sup>2,7</sup>, Jason Flannick<sup>10,11</sup>, Maddalena Trombetta<sup>12</sup>, Enzo  
10   Bonora<sup>12</sup>, Claes B. Wolheim<sup>8</sup>, Leena Sarelin<sup>13</sup>, Riccardo C. Bonadonna<sup>14</sup>, Patrik Rorsman<sup>2</sup>, Guy A  
11   Rutter<sup>9</sup>, Benjamin Davies<sup>7</sup>, Julia Brosnan<sup>6</sup>, Mark I. McCarthy<sup>2,7,15</sup>, Timo Otonkoski<sup>3</sup>, Jens O.  
12   Lagerstedt<sup>5</sup>, Jesper Gromada<sup>4</sup>, Anna L. Gloyn<sup>2,7,15\*</sup>, Tiinamaija Tuomi<sup>1,13,16</sup> and Leif Groop<sup>1,8\*</sup>

13

14    1. Institute for Molecular Medicine Finland (FIMM), Helsinki University, Helsinki, Finland.  
15    2. Oxford Centre for Diabetes Endocrinology & Metabolism, University of Oxford, UK.  
16    3. Research Programs Unit, Molecular Neurology and Biomedicum Stem Cell Centre, Faculty of Medicine,  
17    University of Helsinki, Finland.  
18    4. Regeneron Pharmaceuticals, Tarrytown, New York, USA.  
19    5. Department of Experimental Medical Science, Lund University, 221 84, Lund, Sweden.  
20    6. Pfizer Inc, Cambridge, MA, United States of America.  
21    7. Wellcome Centre for Human Genetics, University of Oxford, UK.  
22    8. Lund University Diabetes Centre, Department of Clinical Sciences, Lund University, Skåne University  
23    Hospital, SE-20502 Malmö, Sweden.  
24    9. Section of Cell Biology, Department of Medicine, Imperial College London, Imperial Centre for Translational  
25    and Experimental Medicine, Hammersmith, Hospital, Du Cane Road, London, W12 0NN, UK.  
26    10. Department of Molecular Biology, Massachusetts General Hospital, Boston, Massachusetts, USA.  
27    11. Program in Medical and Population Genetics, Broad Institute, Cambridge, Massachusetts, USA.

28 12. Department of Medicine, University of Verona and Azienda Ospedaliera Universitaria Integrata of Verona,  
29 Verona, Italy  
30 13. Folkhälsan Research Center, Helsinki, Finland.  
31 14. The Azienda Ospedaliera Universitaria of Parma, 43125 Parma, Italy.  
32 15. Oxford NIHR Biomedical Research Centre, Churchill Hospital, Oxford, UK  
33 16. Abdominal Center, Endocrinology, Helsinki University Central Hospital; Research Program for Diabetes and  
34 Obesity, University of Helsinki, Helsinki, Finland.

35 # These authors contributed equally to the study

36 \*Correspondence: Leif Groop, Institute for Molecular Medicine Finland (FIMM), Helsinki University. Leif.  
37 Groop@helsinki.fi and/or leif.Groop@med.lu.se and Anna L Gloyn, Oxford Centre for Diabetes Endocrinology &  
38 Metabolism, University of Oxford, UK. anna.gloyn@drl.ox.ac.uk

39

40

41

42

43

44

45

46

47

48

49

50

51

52

53

54

55

56

57

58

59

60

61

62

63

64

65

66

67

68

69 **Abstract**

70 A rare loss-of-function variant p.Arg138\* in *SLC30A8* encoding the zinc transporter 8 (ZnT8)  
71 enriched in Western Finland protects against type 2 diabetes (T2D). We recruited relatives of the  
72 identified carriers and showed that protection was associated with better insulin secretion due to  
73 enhanced glucose responsiveness and proinsulin conversion, especially compared with individuals  
74 matched for the genotype of a common T2D risk variant in *SLC30A8*, p.Arg325. In genome-edited  
75 human IPS-derived  $\beta$ -like cells, we establish that the p.Arg138\* variant results in reduced *SLC30A8*  
76 expression due to haploinsufficiency. In human  $\beta$ -cells loss of *SLC30A8* leads to increased glucose  
77 responsiveness and reduced  $K_{ATP}$  channel function, which was also seen in isolated islets from  
78 carriers of the T2D-protective allele p.Trp325. These data position ZnT8 as an appealing target for  
79 treatment aiming at maintaining insulin secretion capacity in T2D.

80

81 **Introduction**

82 Zinc transporters (ZnTs) regulate the passage of zinc across biological membranes out of the  
83 cytosol, while Zrt/Irt-like proteins transport zinc into the cytosol<sup>1</sup>. ZnT8, encoded by *SLC30A8*, is  
84 highly expressed in membranes of insulin granules in pancreatic  $\beta$ -cells, where it transports zinc  
85 ions for crystallization and storage of insulin<sup>2</sup>. We have described a loss-of-Function (LoF) variant  
86 p.Arg138\* (rs200185429, c.412C>T) in the *SLC30A8* gene, which conferred 53% protection  
87 against T2D<sup>3</sup>. This variant was extremely rare (0.02%) in most European countries but more  
88 common (>0.2%) in Western Finland<sup>3</sup>. We also reported a protective frameshift variant  
89 p.Lys34Serfs\*50 conferring 83% protection against T2D in Iceland. A recent (>44K) exome  
90 sequencing study reported >30 alleles in *SLC30A8* reducing the risk of T2D, confirming it as a  
91 robust target for T2D protection<sup>4</sup>. Further, the *SLC30A8* gene also harbors a common variant  
92 (rs13266634, c.973T>A) p.Trp325Arg in the C-terminal domain<sup>5</sup>. While the major p.Arg325 allele  
93 (>70% of the population) confers increased risk for T2D, the minor p.Trp325 allele is protective<sup>6</sup>.

94 The mechanisms by which reduced activity of ZnT8 protect against T2D are largely unknown.  
95 Several attempts have been made to study loss of *Slc30a8* function in rodent models, but the results  
96 have been inconclusive: knock-out of *Slc30a8* led to either glucose intolerance or had no effect in  
97 mice<sup>7,8,9</sup>, while over-expression improved glucose tolerance without effect on insulin secretion<sup>10</sup>. In  
98 a mouse model harbouring the equivalent of the human p.Arg138\* variant we were unable to detect  
99 any ZnT8 protein and observed no effect on glucose<sup>11</sup>. These rodent *in vitro* and *in vivo* experiments  
100 present a complex picture which might not recapitulate the T2D protective effects by *SLC30A8* LoF  
101 mutations in humans. We therefore performed detailed metabolic studies in human carriers of the  
102 LoF variant (p.Arg138\*) recruited on the basis of their genotype, performed comprehensive  
103 functional studies in human  $\beta$ -cell models and compared with the mouse model carrying the human  
104 p.Arg138\*-*SLC30A8* mutation.

105

106

107 **Results**

108 **Recruitment by genotype**

109 Given the enrichment of the p.Arg138\*-*SLC30A8* variant in Western Finland, we genotyped  
110 >14,000 individuals from the Botnia Study<sup>12</sup> for the *SLC30A8* p.Arg138\* mutation and the common  
111 p.Trp325Arg variant (Fig. 1). None of the p.Arg138\* mutation carriers was homozygous for the  
112 protective common variant, p.Trp325 and p.Arg138\* segregated with p.Arg325 in the families  
113 (Supplementary Fig. 1). Thus, we present the data in three different ways: 1) p.Arg138\* *vs.* all  
114 p.Arg138Arg, 2) p.Arg138\* *vs.* p.Arg138Arg having at least one p.Arg325 allele (p.Trp325Arg or  
115 p.Arg325Arg), and 3) p.Arg325 (p.Trp325Arg or p.Arg325Arg) *vs.* p.Trp325Trp on a background  
116 of p.Arg138Arg. We included 79 p.Arg138\* carriers and 103 non-carriers. Of them, 54 p.Arg138\*  
117 and their 47 relatives with p.Arg138Arg participated in a test meal (Fig. 1 and Supplementary Table  
118 1). In addition, 35 p.Arg138\* and 8141 p.Arg138Arg had previously undergone an oral glucose  
119 tolerance test (OGTT, Fig. 1 and Supplementary Table 2).

120 Replicating our previous findings<sup>3</sup>, carriers of p.Arg138\* had reduced risk of T2D (OR=0.40,  
121 P=0.003) in analysis of total 4564 T2D subjects (13 p.Arg138\* carriers) and 8183 non-diabetic (55  
122 p.Arg138\* carriers) individuals. Additionally, non-diabetic p.Arg138\* carriers have lower fasting  
123 glucose concentrations (P=0.033) than p.Arg138Arg. There were no significant differences in  
124 plasma zinc concentrations measured during test meal or OGTT (data not shown).

125 *Comparison of p.Arg138\* vs. p.Arg138Arg:* The p.Arg138\* carriers have lower blood glucose  
126 levels during test meal specifically during the first 40 minutes (P=0.02) and better corrected insulin  
127 response (CIR) (at 20 min, p=0.046) than non-carriers (Fig. 2a and Supplementary Tables 3).  
128 Similarly, the carriers had better insulin response to OGTT (Fig 3b-c, left panel), especially the  
129 early incremental insulin response (p=0.008) and insulin/glucose ratio (at 30 min, p=0.002,

130 Supplementary Tables 4). Of note, the p.Arg138\* carriers had significantly lower proinsulin/C-  
131 peptide (20 min: P=0.041; 40 min: P=0.043) and proinsulin/insulin (20 min: P=0.006) ratios during  
132 test meal suggesting effects on proinsulin conversion (Fig. 2d-e). No differences were seen in  
133 glucagon, GLP-1 or free fatty acids concentrations during test meal (Supplementary Fig. 2c-e).  
134 Neither model-based insulin clearance index nor the ratio of insulin and C-peptide areas under the  
135 curve during test meal differed between p.Arg138\* and p.Arg138Arg, making changes in insulin  
136 clearance<sup>13</sup> unlikely (Supplementary Fig. 2f-g).

137 *Comparison of p.Arg138\* vs. p.Arg138Arg–p.Arg325:* The above differences were magnified when  
138 we restricted the p.Arg138Arg group to carriers of the common risk variant p.Arg325 (middle panel  
139 of Fig. 2). The early phase (0-40 min) insulin (p=0.026), insulin/glucose ratio (p=0.004) and CIR  
140 (p=0.004; 20 min, Supplementary Table 3) were all greater in p.Arg138\* carriers compared with  
141 those having p.Arg138Arg on a background of p.Arg325. Both the proinsulin/C-peptide (20 min:  
142 P=0.027, 40 min: P=0.044) and proinsulin/insulin ratios (20 min: P=0.003) were reduced in  
143 p.Arg138\* carriers (middle panel of Fig. 2d-e).

144 *Comparison of p.Trp325Trp vs. p.Arg325:* The effect of p.Trp325Trp genotype on glucose and  
145 insulin response mimicked the effects of p.Arg138\* with pronounced early (20 min) insulin  
146 (p=0.035) and C-peptide (p=0.025) responses during test meal (right panel of Fig. 2b-c and  
147 Supplementary Fig. 2a), as well as increased insulin secretion (30 min insulin, 30 min  
148 insulin/glucose, incremental insulin, P≤0.003) and lower fasting and 120 minute proinsulin  
149 (p=0.006 and p=0.039, respectively) concentration during OGTT in p.Trp325 carriers  
150 (Supplementary Table 4, right panel of Fig. 3b-c). Moreover, p.Trp325Trp carriers undergoing  
151 intravenous glucose tolerance tests (IVGTT) showed a pronounced (p=0.003) early incremental  
152 insulin secretion response (Supplementary Fig. 3a-b and Supplementary Table 4). In patients with  
153 newly diagnosed T2D, the p.Trp325Trp carriers showed a trend (P=0.12) to enhanced β-cell  
154 sensitivity to glucose during the OGTT (Supplementary Fig. 3c).

155 Taken together, all the human *in vivo* results show that T2D protection by the LoF variant  
156 p.Arg138\* is due to enhanced glucose-stimulated insulin secretion combined with enhanced  
157 proinsulin conversion. The common T2D protective allele p.Trp325 shows a similar – albeit weaker  
158 - metabolic phenotype suggesting it might also reduce ZnT8 function.

159 ***SLC30A8* p.Arg138\* variant in human iPSCs**

160 The majority of nonsense *SLC30A8* alleles (including p.Arg138\*) protecting against T2D are  
161 located in the first four exons of the eight-exon canonical islet *SLC30A8* transcript  
162 ENST00000456015 and are predicted to undergo nonsense mediated decay (NMD), a cell  
163 surveillance pathway which reduces errors in gene expression by eliminating mRNA transcripts that  
164 contain premature stop codons. To confirm that the p.Arg138\* allele indeed leads to  
165 haploinsufficiency through NMD, we used CRISPR-Cas9 to introduce the p.Arg138\* variant into  
166 the *SLC30A8* locus of the SB Ad3.1 human iPSC cell line (Supplementary Fig. 4a, Methods). Two  
167 hiPSC lines for the p.Arg138\*-SLC30A8 variant (Clone B1 and A3) were generated and compared  
168 to an unedited p.Arg138Arg-SLC30A8 CRISPR hiPSC line. Both B1 and A3 clones were  
169 heterozygous with mono-allelic sequencing confirming the p.Arg138\* variant in only one allele  
170 (Supplementary Fig. 4b). All hiPSC lines passed quality control checks including karyotyping and  
171 pluripotency (Supplementary Fig. 4c).

172 Accordingly, we subjected our *SLC30A8*-edited iPSCs to a previously published *in vitro* endocrine  
173 pancreas differentiation protocol<sup>14</sup> (Supplementary Fig. 4d-k, Methods). At the end of the seven  
174 stage protocol, *SLC30A8* expression was significantly reduced in cells heterozygous for the  
175 p.Arg138\* allele (clone B1 0.09±0.04; clone A3 0.08±0.05) compared to unedited control cells  
176 (1.03±0.11) (Fig. 4a). Of note, p.Arg138\* allele specific *SLC30A8* expression was reduced  
177 compared to the WT allele<sup>15</sup> (clone B1: 22.9±2.1%; clone A3: 26.0±3.9%) (Fig. 4b-c). Inhibition of  
178 NMD by cyclohexamide increased expression of the p.Arg138\* transcript more than the  
179 p.Arg138Arg transcript compared to DMSO control (clone B1: 209±52% and clone A3: 199±67%

180 vs. clone B1: 161±30% and clone A3: 132±35%, respectively, Fig. 4d-e). Taken together, these data  
181 show that the protective p.Arg138\*-*SLC30A8* allele undergoes NMD, resulting in  
182 haploinsufficiency for *SLC30A8*.

183 **Impact of *SLC30A8* loss in a human  $\beta$ -cell line**

184 Since human *in vivo* studies provided strong evidence for a role of the p.Arg138\* on insulin  
185 secretion and proinsulin processing, we studied the impact of *SLC30A8* loss using siRNA mediated  
186 knock down (KD) on both phenotypes in a well characterized human  $\beta$ -cell model EndoC- $\beta$ H1<sup>16</sup>  
187 (Methods). By siRNA, we achieved 55-65% decrease in *SLC30A8* mRNA (p=0.008) and protein  
188 (p=0.016, Fig. 5a-c).

189 KD of *SLC30A8* had no significant effect on glucose- or tolbutamide-stimulated insulin secretion or  
190 on insulin content (Fig. 5d-e) but basal insulin secretion was higher in si*SLC30A8* transfected cells  
191 compared to scrambled siRNA cells (p=0.012, Fig. 5d), and the inhibitory effect of diazoxide, a  
192 K<sub>ATP</sub> channel opener, on glucose-stimulated insulin secretion was reduced (p=2×10<sup>-3</sup>, Fig. 5d). We  
193 measured the resting membrane conductance (G<sub>m</sub>), which principally reflects K<sub>ATP</sub> channel activity.  
194 In control cells, G<sub>m</sub> was in agreement with that previously reported<sup>17</sup>. *SLC30A8* KD reduced G<sub>m</sub> by  
195 65% (p=0.002, Fig. 5f) without effect on cell size (Fig. 5g), an effect that correlated with reduced  
196 expression of the two genes encoding the K<sub>ATP</sub> channel subunits SUR1 (*ABCC8*) and Kir6.2  
197 (*KCNJ11*) (Fig. 5h). However, insulin secretion elicited by increasing extracellular K<sup>+</sup> ([K<sup>+</sup>]<sub>o</sub>) to 50  
198 mM (to depolarise the cells and open voltage-gated Ca<sup>2+</sup> channels) and 16.7 mM glucose was  
199 significantly higher after *SLC30A8* KD (p=0.008, Fig. 5i). The proinsulin-insulin ratios (both total  
200 and secreted hormones) were decreased in si*SLC30A8* cells (p<0.001, Fig. 5j-k). Although mRNA  
201 of the proinsulin processing genes *PC1/3* and *CPE* was decreased, we could not detect a similar  
202 reduction at the protein level (Fig. 5l-n).

203 RNA sequencing of *SLC30A8* KD cells (n=3 vs. 3) replicated the reduction of *KCNJ11* and *ABCC8*  
204 gene expression (p=4.3 x10<sup>-3</sup> and p=2.9x10<sup>-5</sup>, respectively). In addition, expression of genes  
205 involved in regulation of  $\beta$ -cell excitability was down-regulated, including *KCNMA1* encoding a  
206 Ca<sup>2+</sup>-activated K<sup>+</sup> channel<sup>18</sup> and *TMTC1* (p=6.8x10<sup>-5</sup> and 2.9x10<sup>-16</sup>, respectively) encoding an ER  
207 adapter protein influencing intracellular calcium levels. Also, expression of genes associated with  
208  $\beta$ -cell maturation and secretion was influenced by *SLC30A8* KD with decreased expression of  
209 *NKX6.1* and *PDX1* and increased expression of *SOX4*, *SOX6* and *SOX11* (Fig. 5o-p).  
  
210 In addition, we also observed increased AKT phosphorylation (pAKT-473) and improved cell  
211 survival under ER stress (p<0.017, Fig. 5q-s), mechanisms which also could contribute to the  
212 overall protection by preserving  $\beta$ -cell mass<sup>19</sup>. Taken together, these data generated by disrupting  
213 *SLC30A8* in a human  $\beta$ -cell pointed at multiple mechanisms including changes in proinsulin  
214 conversion, K<sub>ATP</sub> channel activity and cell viability.

215 **Metabolic phenotype of mice carrying the human *SLC30A8* p.Arg138\***

216 Since neither global nor tissue specific *Slc30a8* KD mouse models have recapitulated the human  
217 phenotype in carriers of the *SLC30A8* p.Arg138\* variant, we tried to overcome this problem by  
218 using a mouse model carrying the *Slc30a8* p.Arg138\* variant<sup>11</sup>. These mice do not express the  
219 truncated ZnT8 protein<sup>11</sup>. On a standard chow diet there was no evidence for enhanced insulin  
220 secretion<sup>11</sup>. However, we examined whether they might do so on a high fat diet (HFD). This was  
221 indeed the case (Fig. 6a-h), and the same differences in proinsulin/insulin and proinsulin/C-peptide  
222 ratios were seen as in humans. No changes were seen in insulin clearance.

223 **Impact of p.Arg138\* on protein localization and cytosolic zinc distribution in INS-1 cells**

224 Although we found no evidence in either mouse or our human  $\beta$ -cell model to support the presence  
225 of a truncated protein we explored the possibility of what might happen if a truncated protein  
226 resulted from mRNA evading NMD. Transient overexpression of tagged ZnT8-p.Arg138\* fusion

227 proteins in a rat insulinoma cell line, INS-1e, showed distinct punctate distribution patterns,  
228 consistent with localization of the truncated ZnT8 protein to secretory granules, as previously  
229 observed with the full length protein<sup>20</sup> (Supplementary Fig. 5a-c) Additionally, Western blot  
230 showed stable expression of truncated ZnT8 in native INS1e cells (Supplementary Fig. 5d).  
231 To investigate the effects of a truncated ZnT8 protein on cytosolic free Zn<sup>2+</sup>, we used a genetically-  
232 encoded Zn<sup>2+</sup> sensor eCALWY-4<sup>21</sup>. Overexpression of the truncated protein (p.Arg138\*) had no  
233 impact on cytosolic free Zn<sup>2+</sup> when expressed in INS-1 WT cells ruling out a dominant negative  
234 effect for the truncated protein (Supplementary Fig. 5e-h).

235 **Influence of common *SLC30A8* variants p.Trp325Arg in primary human islets**

236 While adult human islets show high levels of *SLC30A8* expression there was no reproducible effect  
237 of the p.Arg325Trp variant on *SLC30A8* expression in human islets from cadaveric donors (Fig.  
238 7a). Islets obtained from cadaveric p.Trp325 carriers secreted more insulin than p.Arg325Arg  
239 carriers (Fig. 7b-e). The increased glucose responsiveness was observed at submaximal glucose  
240 stimulation (6 mM) rather than at maximal glucose stimulation (16.7 mM) (Fig. 7b-c). Increasing  
241 glucose from 1 mM to 6 mM stimulated insulin secretion 2.2- and 2.7-fold in p.Arg325 and  
242 p.Trp325 carriers respectively, with no effect on insulin content (Fig. 7c-d). This secretion pattern  
243 echoes the one observed after siRNA of *SLC30A8* KD in EndoC-βH1. Insulin secretion in p.Trp325  
244 carriers was also increased at high glucose (16.7 mM) when co-exposed to depolarizing [K<sup>+</sup>]<sub>o</sub> (70  
245 mM) (Fig. 7e) as also seen after *SLC30A8* KD in EndoC-βH1.

246 As *SLC30A8* is highly expressed in human alpha cells<sup>1</sup>, we also measured glucagon secretion from  
247 the same islets (Fig. 7f). In islets from p.Arg325Arg donors, 6 mM glucose inhibited glucagon  
248 secretion by ~50% compared to 1 mM glucose. In islets from p.Trp325Arg donors, glucagon  
249 secretion at 1 mM glucose was reduced by 50% compared to p.Arg325Arg donors with no effect on  
250 glucagon content (Fig. 7f-g).

251 We also explored whether the p.Trp325Arg variant would have trans-eQTL effects on genes  
252 involved in insulin production and secretion<sup>22</sup> (Fig. 7a). Expression of *PCSK1* (P=0.041)  
253 and *PCSK2* (P=0.045) were reduced. Among the genes encoding for K<sub>ATP</sub> channels subunits  
254 only *ABCC8* (P=0.049) expression was significantly affected in islets from p.Trp325 carriers  
255 compared to non-carriers (Fig. 7a). Taken together, the data suggest the common T2D-protective  
256 allele (p.Trp325) may improve the response to a glucose challenge by enhancing insulin secretion  
257 and possibly by reducing glucagon secretion in primary human islets.

258 **Discussion**

259 The current study demonstrates the strengths of using human models for studying the consequences  
260 of LoF mutations in humans, particularly by demonstrating a stronger protective effect of  
261 p.Arg138\* in individuals carrying the common risk p.Arg325 allele on the same haplotype.  
262 However, the minor p.Trp325 allele was also associated with protection against T2D albeit less  
263 pronounced. This emphasizes the importance of taking into account the genetic background of the  
264 human LoF carrier.

265 Whilst the data from all our sub-studies are consistent with increased glucose responsiveness, the  
266 precise molecular mechanisms for these phenotypes, involvement of zinc and an explanation for  
267 why there are discrepancies between humans and rodents remain elusive. In the IPS-derived beta-  
268 like cells, the p.Arg138\* variant dramatically lowered expression with evidence of NMD resulting  
269 in haploinsufficiency. Similarly, in the mouse model we were unable to detect the truncated  
270 protein, but we could detect appreciable levels of RNA<sup>11</sup>.

271 The most reproducible finding in all sub-studies of p.Arg138\* was enhanced glucose-stimulated  
272 insulin secretion accompanied by increased conversion of proinsulin to C-peptide and insulin.  
273 Carriers of p.Trp325 displayed a similar phenotype, which is in line with a previous study showing  
274 impaired proinsulin conversion in carriers of the risk p.Arg325 allele<sup>23</sup>. There could also be other

275 potential explanations for this effect, as it has been suggested that it takes some time for insulin to  
276 mature and become biologically active<sup>24,25</sup>. It is possible that the pronounced effects of the LoF  
277 mutation at 20 and 40 min of test meal could reflect such a mechanism.

278 The present and previous studies demonstrate that loss of ZnT8 function after silencing the murine  
279 gene reduces total cellular zinc content as well as free Zn<sup>2+</sup> in the cytosol and granules<sup>7,10,20,26</sup>. LoF  
280 p.Arg138\* (assuming no or minimal escape from NMD) is therefore likely to exert the same effects  
281 on intracellular zinc concentrations and may thus impact insulin secretion through intracellular  
282 mechanisms, including potential differences in Zn<sup>2+</sup> secretion. Also, a recent study showed that the  
283 p.Arg325Arg variant was associated with higher islet zinc concentrations<sup>27</sup>. In the present study  
284 over-expression of the LoF mutation p.Arg138\* in INS-1 cells did not result in changes in cytosolic  
285 zinc concentrations leaving a reduction of zinc in insulin granules as a plausible explanation which  
286 still needs to be experimentally confirmed.

287 In support of a protective effect of lowering intracellular zinc concentrations on development of  
288 diabetes, in the CNS, Zn<sup>2+</sup> plays an important role as a regulator of cellular excitability<sup>28</sup> and Zn<sup>2+</sup>  
289 has been reported to activate K<sub>ATP</sub> channels<sup>29</sup>, inhibit L-type voltage-gated Ca<sup>2+</sup> channels and inhibit  
290 insulin secretion<sup>30</sup>.

291 Taken together, our data consistently demonstrate that heterozygosity for a LoF mutation  
292 p.Arg138\* and homozygosity for a common variant p.Trp325Trp of the *SLC30A8* are associated  
293 with increased insulin secretion capacity and lower risk of T2D without any negative effect.  
294 Therefore, ZnT8 remains an appealing safe target for antidiabetic therapy preserving β-cell  
295 function.

296

297

298

299 **Methods**

300 **Human study population**

301 The Botnia Study has been recruiting patients with T2D and their family members in the area of  
302 five primary health care centers in western Finland since 1990. Individuals without diabetes at  
303 baseline (relatives or spouses of patients with T2D) have been invited for follow-up examinations  
304 every 3-5 years<sup>12</sup>. The Prevalence, Prediction and Prevention of diabetes (PPP)–Botnia Study is a  
305 population-based study in the same region including a random sample of 5,208 individuals aged 18  
306 to 75 years from the population registry<sup>31</sup>. Diabetes Registry Vaasa (DIREVA) is regional diabetes  
307 registry of > 5000 diabetic patients from Western Finland (Botnia region)<sup>32</sup>. In the current study, we  
308 included >14,000 individuals (Botnia family study=5678, PPP=4862, and DIREVA=3835). All  
309 participants gave their written informed consent and the study protocol was approved by the Ethics  
310 Committee of Helsinki University Hospital, Finland (the Botnia studies) and the Ethics Committee  
311 of Turku University Hospital (DIREVA).

312 **Oral Glucose Tolerance Test (OGTT) and test meal:** Subjects maintained a weight-maintaining  
313 diet and avoided vigorous exercise for 3 days prior to the OGTT or test meal, which were  
314 performed after an overnight fast. Height, weight, hip and waist circumferences, fat percentage (%,  
315 bioimpedance analyzer) and blood pressure (sitting, 3 measurements after 5 min rest) were  
316 measured. The participants ingested 75 g dextrose (in a couple of minutes, OGTT) or a 526 kcal  
317 mixed meal (in 10 minutes, test-meal: 76 g carbohydrate, 17 g protein and 15 g fat). Blood samples  
318 were drawn from an antecubital vein for plasma (P-) glucose and serum (S-) insulin and C-peptide  
319 at 0, 30, 120 min during the OGTT; for P-glucose, P-glucagon, S- insulin, S-C-peptide, S-zinc, and  
320 total S-GLP-1 at 0, 20, 40, 70, 100, 130, 160 and 190 min during the test meal. Test meal samples  
321 for S-FFA were collected at 0, 40 and 120 min and for S-proinsulin at 0, 20, 40 and 130 min,  
322 respectively. Urine was collected between 0 – 70 and 70 – 190 min for the determination of glucose  
323 and zinc excretion during the test meal.

324 **Intravenous Glucose Tolerance Test (IVGTT):** IVGTT group consists of total 849 (male- 403,  
325 female- 446) individuals with an average age of 51 years. An antecubital polyethylene catheter was  
326 placed to one hand for the infusion of 0.3 g/kg body weight of glucose (maximum dose 35 g)  
327 intravenously for 2 min. A retrogradely positioned wrist vein catheter was placed in the other hand,  
328 held in a heated (70°C) box in order to arterialize the venous blood. Arterialized blood samples  
329 were drawn at 0, 2, 4, 6, 8,10, 20, 30, 40, 50 and 60 min for P-glucose and S-insulin.

330 **Biochemical measurements:** P-glucose was analyzed using glucose oxidase (Beckman Glucose  
331 Analyzer, Beckman Instruments, Fullerton, CA, USA; Botnia Family Study) or glucose  
332 dehydrogenase method (Hemocue, Angelholm, Sweden; PPP-Botnia and test meal studies). In the  
333 Botnia Family study, S-insulin was measured by radioimmunoassay (RIA, Linco; Pharmacia,  
334 Uppsala, Sweden), enzyme immunoassay (EIA; DAKO, Cambridgeshire, U.K.) or  
335 fluoroimmunometric assay (FIA, AutoDelfia; Perkin Elmer Finland, Turku, Finland). For the  
336 analysis, insulin concentrations obtained with different assays were transformed to cohere with  
337 those obtained using the EIA. The correlation coefficient between RIA and EIA as well as between  
338 FIA and EIA was 0.98 ( $P < 0.0001$ ). S-insulin was measured by the FIA in baseline visit of PPP-  
339 Botnia and the test meal study (correlation coefficient 0.98). S-proinsulin was measured using RIA  
340 (Linco; Pharmacia, Uppsala, Sweden, OGTT data) or EIA (Mercodia AB, Uppsala, Sweden; test-  
341 meal data), and P-glucagon using RIA (EMD Millipore, St. Charles, MO; OGTT data) or EIA  
342 (Mercodia AB, Uppsala, Sweden; test-meal data). S-FFA was measured by an enzymatic  
343 colorimetric method (Wako Chemicals, Neuss, Germany). Serum total cholesterol, HDL and  
344 triglyceride concentrations were measured with Cobas Mira analyzer (Hoffman LaRoche, Basel,  
345 Switzerland), and since 2006 with an enzymatic method (Konelab 60i analyser; Thermo Electron  
346 Oy, Vantaa, Finland). Serum LDL cholesterol was calculated using the Friedewald formula. Blood  
347 collected in tubes containing DPP4-inhibitors was used for radioimmunoassay<sup>33</sup> for total P-GLP-1  
348 (intact GLP-1 and the metabolite GLP-1 9-36 amide) during test meal.

349 Serum and urine samples for zinc were collected in trace element tubes (Beckton Dickinson, NJ,  
350 USA) and S- and U-zinc analyzed by two commercial laboratories: NordLab (Oulu, Finland; atom  
351 absorption spectrophotometry, AAS) until 6<sup>th</sup> May 2015, then in Synlab (Helsinki, Finland; AAS  
352 for serum, mass spectrophotometry ICP-MS for U-zinc). The S-zinc concentrations were corrected  
353 for P-albumin ( $r = 0.34$ ,  $p = 0.008$  Nordlab,  $r = 0.34$ ,  $p = 0.03$  Synlab).

354 Corrected insulin response (CIR) was calculated for test meal (at 20 min) and OGTT (at 30 min.)  
355 using the formula  $CIR(t) = Ins(t) / [Gluc(t) \cdot (Gluc(t)-3.89)]$ , where  $Ins(t)$  and  $Gluc(t)$  are insulin (in  
356 mU/L) and glucose concentrations (in mmol/L) at sample time point  $t$  (min)<sup>34</sup>. Estimation of Insulin  
357 clearance index was done on the model based estimation of glucose-, insulin- and C-peptide curves  
358 during the test meal using the equation  $AUC(ISR) / [(AUC(ins)+(I(basal)-I(final)) \cdot MRT(ins))]$ ,  
359 where  $AUC(ISR)$  is the area under the curve of insulin secretion rate,  $AUC(ins)$  is the area under  
360 the curve of insulin concentration,  $I(final)$  is insulin concentration at the end, and  $I(basal)$  insulin  
361 concentration at the beginning of the study<sup>35</sup>.  $MRT(ins)$  is the mean residence time of insulin, and  
362 was assumed to be 27 minutes as reported previously<sup>36</sup>.

363 **Genotyping:** We analyzed genotype data for rs13266634 (p.Trp325Arg) and rs200185429  
364 (p.Arg138\*) for three cohorts genotyped with different genome-/exome-wide chips: the Botnia  
365 family cohort (Illumina Global Screening array-24v1, genotyped at Regeneron Pharmaceuticals),  
366 PPP-Botnia (Illumina HumanExome v1.1 array, genotyped at Broad Institute<sup>3</sup>) and DIREVA  
367 (Illumina Human CoreExome array-24v1, genotyped at LUDC). For the Botnia family cohort,  
368 genotype data for p.Arg138\* were imputed (info score >0.95) from the available GWAS data by  
369 phasing using SHAFT-IT v2<sup>37</sup> and imputing using the GoT2D reference panel<sup>38</sup> by IMPUTEv2<sup>39</sup>.  
370 The carrier status of imputed p.Arg138\* was additionally confirmed from exome sequencing data.  
371 Genotyping (p.Trp325Arg and p.Arg138\*) the family members participating in the genotype based  
372 recall study (test meal study) was performed using TaqMan (Applied Biosystems, Carlsbad, CA).  
373 The genotype distribution of both variants was in accordance with Hardy-Weinberg equilibrium in

374 all the cohorts. We did not detect any Mendelian errors in the families.

375 ***Genetic Association Analysis:*** All the quantitative traits were inversely normally transformed  
376 before the analyses. The family-based recall study included only non-diabetic subjects during test  
377 meal and analysis of data was performed using family-based association analyses adjusting for age,  
378 sex, BMI, and other covariates if appropriate, using QTDT (v2.6.1)<sup>40</sup>. The significance levels were  
379 derived from 100,000 permutations as implemented in QTDT. Also, the OGTT study included only  
380 non-diabetic subjects. The association analysis was performed using mixed linear model  
381 considering genetic relatedness among samples as implemented in GCTA (v1.91)<sup>41</sup>.

382 ***Study participants and their clinical measurements in Verona Newly Diagnosed Diabetes Study***  
383 ***(VNDS):*** The Verona Newly Diagnosed Type 2 Diabetes Study (VNDS; NCT01526720) is an  
384 ongoing study aiming at building a biobank of patients with newly diagnosed (within the last six  
385 months) type 2 diabetes. Patients are drug-naïve or, if already treated with antidiabetic drugs,  
386 undergo a treatment washout of at least one week before metabolic tests are performed<sup>42</sup>. Each  
387 subject gave informed written consent before participating in the research, which was approved by  
388 the Human Investigation Committee of the Verona City Hospital. Metabolic tests were carried out  
389 on two separate days in random order<sup>42</sup>. Plasma glucose concentration was measured in duplicate  
390 with a Beckman Glucose Analyzer II (Beckman Instruments, Fullerton, CA, USA) or an YSI 2300  
391 Stat Plus Glucose&Lactate Analyzer (YSI Inc., Yellow Springs, OH, USA) at bedside. Serum C-  
392 peptide and insulin concentrations were measured by chemiluminescence as previously described<sup>42</sup>.  
393 The analysis of the glucose and C-peptide curves during the OGTT was carried out with a  
394 mathematical model as described previously<sup>42</sup>. This model was implemented in the SAAM 1.2  
395 software (SAAM Institute, Seattle, WA) to estimate its unknown parameters. Numerical values of  
396 the unknown parameters were estimated by using nonlinear least squares. Weights were chosen  
397 optimally, i.e., equal to the inverse of the variance of the measurement errors, which were assumed  
398 to be additive, uncorrelated, with zero mean, and a coefficient of variation (CV) of 6-8%. A good fit

399 of the model to data was obtained in all cases and unknown parameters were estimated with good  
400 precision. In this paper we report the response of the beta cell to glucose concentration  
401 (proportional control of beta cell function), which in these patients accounts for  $93.2 \pm 0.3\%$  of the  
402 insulin secreted by the beta cell in response to the oral glucose load. Genotypes were assessed by  
403 the high-throughput genotyping Veracode technique (Illumina Inc, CA), applying the GoldenGate  
404 Genotyping Assay according to manufacturer's instructions. Hardy-Weinberg equilibrium was  
405 tested by chi-square test. Variant association analyses were carried out by generalized linear models  
406 (GLM) as implemented in SPSS 25.0 and they were adjusted for a number of potential confounders,  
407 including age, sex and BMI.

408 **iPSC generation, differentiation and genome editing**

409 ***iPSC generation and maintenance:*** The human induced pluripotent stem cell line (hiPSC) SB  
410 Ad3.1 was previously generated and obtained through the IMI/EU sponsored StemBANCC  
411 consortium via the Human Biomaterials Resource Centre, University of Birmingham  
412 (<http://www.birmingham.ac.uk/facilities/hbrc>). Human skin fibroblasts were obtained from a  
413 commercial source (Lonza CC-2511, tissue acquisition number 23447). They had been collected  
414 from a Caucasian donor with no reported diabetes with fully informed consent and with ethical  
415 approval from the National Research Ethics Service South Central Hampshire research ethics  
416 committee (REC 13/SC/0179). The fibroblasts were reprogrammed to pluripotency as previously  
417 described<sup>43</sup> and were subjected to the following quality control checks: SNP-array testing via  
418 Human CytoSNP-12v2.1 beadchip (Illumina #WG-320-2101), DAPI-stained metaphase counting  
419 and mFISH, flow cytometry for pluripotency markers (BD Biosciences #560589 and 560126), and  
420 mycoplasma testing (Lonza #LT07-118).

421 ***CRISPR-Cas9 mediated generation of p.Arg138\* human induced pluripotent stem cell line:***

422 Several guide RNAs (gRNAs) were designed using MIT CRISPR tool (<http://crispr.mit.edu/>) to  
423 target near exon 3 of *SLC30A8* (ENST00000456015). The gRNAs were also subjected to an

424 additional BlastN search ([www.ensembl.org](http://www.ensembl.org)) to confirm specificity and identified no additional off-  
425 target sites. The gRNA (AGCAGGTACGGTTCATAGAG) was sub-cloned into the *BsbI* restriction  
426 sites in pX330<sup>44</sup> plasmid that was previously modified to contain a puromycin selection cassette.  
427 Single strand oligonucleotides for homology-directed repair (HDR) were synthesised by  
428 Eurogentec, stabilised by addition of a phosphorothioate linkage at the 5' end, and contained two  
429 nucleotide changes: i) the T2D-protective nonsense mutation at codon-138 (c.412C>T, p.Arg138\*),  
430 which also mutated the PAM sequence, and ii) a silent missense mutation at codon-139 (c.417A>T,  
431 p.Ala139Ala) to introduce an *AluI* restriction site for genotyping.  
432 Human iPSCs were co-transfected with *SLC30A8*-px330-puromycin resistant vectors and HDR  
433 oligos using Fugene6 according to manufacturer's guidelines (Promega #E2691). Following  
434 transient puromycin-selection, single clones were picked and expanded as described previously<sup>45</sup>.  
435 Genotyping PCR was performed using primers (Forward: TACCCCAGGAATGGCTTCTC;  
436 Reverse: ACGTGTCCTGTTGTCCC) to amplify targeted region followed by *AluI* restriction  
437 digest. Successfully targeted clones were confirmed via Sanger sequence and monoallelic  
438 sequencing was performed by TA-cloning (pGEM®-T Easy Vector System; Promega #A1360) of  
439 the PCR amplicons. The control hiPSC line (p.Arg138Arg) was generated from hiPSC cells that  
440 went through the CRISPR pipeline without being edited at the *SLC30A8* locus. The two p.Arg138\*  
441 clones (A3 and B1) and the unedited control line (p.Arg138Arg) passed quality control checks that  
442 included repeat chromosome counting and pluripotency testing.  
443 ***In vitro differentiation of hiPSCs towards Beta-like cells:*** Directed differentiation of hiPSCs  
444 towards beta-like cells was performed using a previously published protocol<sup>14,46</sup>. hiPSCs were  
445 seeded on Growth Factor Reduced Matrigel-coated CellBind 12-well tissue culture plates (Corning  
446 #356230 & #3336) at a cell density of 1.3x10<sup>6</sup> in mTesR1 (Stem Cell Technologies #05850) with  
447 10 µM Y-27632 dihydrochloride (Abcam #ab120129). The following morning, hiPSCs were fed  
448 mTesR1 media >4 hours before starting the seven-stage differentiation protocol.

449 *Stage 1 (Definitive Endoderm):* Cells were washed once with PBS before adding 0.5% bovine  
450 serum albumin (BSA; Roche #10775835001) MCDB131 media [(ThermoFisher Scientific  
451 #10372019) containing 1x Penicillin-Streptomycin (Sigma #P0781), 1.5 g/L sodium bicarbonate  
452 (ThermoFisher Scientific #25080060), 1x GlutaMAX™ (ThermoFisher Scientific #35050038) and  
453 10 mM Glucose (ThermoFisher Scientific #A2494001)] supplemented with 100 ng/mL Activin A  
454 (Peprotech #120-14) and 3  $\mu$ M CHIR 99021 (Axon Medchem #1386). On day 2 and 3, cells were  
455 cultured with 0.5% BSA MCDB131 media supplemented with either 100 ng/mL Activin A and 0.3  
456  $\mu$ M CHIR 99021 (day 2) or with 100 ng/mL Activin A alone (day 3).  
  
457 *Stage 2 (Primitive Gut Tube):* Cells were cultured for 48 hours in 0.5% BSA MCDB131 media with  
458 0.25 mM ascorbic acid (Sigma #A4544) and 50 ng/mL KGF (PeproTech #100-19).  
  
459 *Stage 3 (Posterior Foregut):* Cells were cultured for two days in 2% BSA MCDB131 media  
460 supplemented with 1 g/L sodium bicarbonate, 0.25 mM ascorbic acid, 0.5x Insulin-Transferrin-  
461 Selenium-Ethanolamine (ITS-X; ThermoFisher Scientific #51500056), 1  $\mu$ M retinoic acid (RA;  
462 Sigma-Aldrich #R2625), 0.25  $\mu$ M Sant-1 (Sigma-Aldrich #S4572), 50 ng/ml KGF, 100 nM  
463 LDN193189 (Stemgent #04-0074), and 100 nM  $\alpha$ -Amyloid Precursor Protein Modulator (Merck  
464 #565740).  
  
465 *Stage 4 (Pancreatic Endoderm):* Cells were cultured for three days in 2% BSA MCDB131 media  
466 supplemented with 1 g/L sodium bicarbonate, 0.25 mM ascorbic acid, 0.5x ITS-X, 0.1  $\mu$ M RA, 0.25  
467  $\mu$ M Sant-1, 2 ng/ml KGF, 200 nM LDN193189 and 100 nM  $\alpha$ -Amyloid Precursor Protein  
468 Modulator.  
  
469 *Stage 5 (Endocrine Progenitors):* Cells remained in planar culture for three days in 2% BSA  
470 MCDB131 media supplemented with 20 mM final glucose, 0.5x ITS-X, 0.05  $\mu$ M RA, 0.25  $\mu$ M  
471 Sant-1, 100 nM LDN193189, 10  $\mu$ M ALK5 Inhibitor II (Enzo Life Sciences #ALX-270-445), 1  $\mu$ M

472 3,3,5-Triiodo-L-thyronine sodium salt (T3; Sigma-Aldrich #T6397), 10  $\mu$ M zinc sulfate  
473 heptahydrate (Sigma # Z0251), and 10  $\mu$ g/mL heparin sodium salt (Sigma #H3149).

474 **Stage 6 (Endocrine Cells):** Cells remained in planar culture for six days in 2% BSA MCDB131  
475 media supplemented with 20 mM final glucose, 0.5x ITS-X, 100 nM LDN193189, 10  $\mu$ M ALK5  
476 Inhibitor II, 1  $\mu$ M T3, 10  $\mu$ M zinc sulfate heptahydrate, and 100 nM  $\gamma$ -Secretase Inhibitor XX  
477 (Merck Millipore #565789).

478 **Stage 7 (Beta-like Cells):** Cells remained in planar culture for another six days in 2% BSA  
479 MCDB131 media supplemented with 20 mM final glucose, 0.5x ITS-X, 10  $\mu$ M ALK5 Inhibitor II,  
480 1  $\mu$ M T3, 1 mM N-Cys (Sigma-Aldrich #A9165), 10  $\mu$ M Trolox (EMD Millipore #648471), 2  $\mu$ M  
481 R248 (SelleckChem #S2841), and 10  $\mu$ M zinc sulfate heptahydrate.

482 ***Quantification of SLC30A8 gene expression in Beta-like Cells derived from CRISPR-edited***  
483 ***hiPSCs:*** Expression of *SLC30A8* was measured at the end of stage 7 using quantitative PCR  
484 (qPCR). Briefly, RNA was extracted using TRIzol Reagent (Life Technologies #15596026)  
485 according to manufacturer's instructions. cDNA was amplified using the GoScript Reverse  
486 Transcription Kit (Promega #A5000). qPCR was performed using 40 ng of cDNA, TaqMan® Gene  
487 Expression Master Mix (Applied Biosystems #4369017) and primer/probes for *SLC30A8*  
488 (Hs00545182\_m1) or the housekeeping gene *TBP* (Hs00427620\_m1). Gene expression was  
489 determined using the  $\Delta\Delta CT$  method by first normalizing to *TBP* and then to the control  
490 p.Arg138Arg sample (n=6-7 wells from two differentiations).

491 ***Allele-specific SLC30A8 expression in Beta-like Cells derived from CRISPR-edited hiPSCs:***  
492 Stage 7 cells were treated with 100  $\mu$ g/mL cycloheximide (Sigma #C4859) or DMSO (Sigma  
493 #D2650) for four hours at 37°C<sup>47</sup> before harvesting for RNA and cDNA synthesis as above. Allele  
494 specific expression was measured using the QX10 Droplet Digital PCR System and C1000 Touch  
495 Thermal Cycler according to manufacturer's guidelines (Bio-Rad). Custom primers and probes for

496 the detection of p.Arg138\* variant were designed using Primer3Plus (Applied Biosystems):  
497 Forward primer AGTCTCTTCTCCCTGTGGTT; Reverse primer  
498 ATGATCATCACAGTCGCCTG; FAM probe 5'-FAM-ATGGCACCGAGCTGA-MGB-3'; VIC  
499 probe 5'-VIC-ATGGCACTGAGCTGAGA-MGB-3'. Results were analysed using Quanta Soft  
500 software (Bio-Rad) and presented as a ratio of wildtype to HDR-edited allele expression (n>3 wells  
501 from two differentiations).

502 **EndoC- $\beta$ H1 culture**

503 The results obtained in EndoC- $\beta$ H1 are from two distinct teams (Helsinki and Oxford) with  
504 different batches of EndoC- $\beta$ H1 cultures. Here, we report both methods and specify for each  
505 experiment the origin of the culture (Helsinki or Oxford). EndoC- $\beta$ H1 cells were cultured in  
506 medium and grown on a matrix as described previously<sup>48</sup> and tested negative for mycoplasma.

507 ***SLC30A8* knockdown in EndoC- $\beta$ H1 cells:** In Oxford, EndoC- $\beta$ H1 cells were transfected with 10  
508 nM siRNA (either SMARTpool ON-TARGETplus SLC30A8 or scramble [Dharmacon #L-007529-  
509 01]) and Lipofectamine RNAiMAX (Life Technologies #13778-075) according to manufacturer's  
510 instructions for a total of 72 hours. In Helsinki, EndoC- $\beta$ H1 cells were transfected using  
511 Lipofectamin RNAiMAX (life technologies). 20nM siRNA ON-TARGETplus siRNA SMARTpool  
512 for human *SLC30A8* gene (Dharmacon; L-007529-01) and ON-TARGETplus Non-targeting pool  
513 (siNT or Scramble) (Dharmacon; D-001810-10-05) were used following the protocol as described  
514 previously<sup>49</sup>. Cells were harvested 96 h post-transfection for further studies.

515 ***Insulin secretion measurements in EndoC- $\beta$ H1 cells:*** In Oxford, cells were subjected to static  
516 insulin secretion assays 72hrs after siRNA transfection as described previously<sup>50</sup>, apart from the  
517 following modifications: cells were stimulated for 1 hr with 1 mM glucose, 20 mM glucose, 1 mM  
518 glucose + 200  $\mu$ M tolbutamide, or 20 mM glucose + 500  $\mu$ M diazoxide. Insulin levels were  
519 measured in both supernatants and cells using the Insulin (human) AlphaLISA Detection Kit and

520 EnSpire Alpha Plate Reader (Perkin Elmer #AL204C and #2390-0000, respectively). Cell count per  
521 well was measured via CyQUANT Direct Cell Proliferation Assay (Thermo Fisher# C35011). Data  
522 are presented as insulin secretion normalized to percentage of insulin content from Control  
523 condition. RNA extraction, cDNA synthesis, and qRT-PCR was performed as above (*SLC30A8*  
524 gene expression in CRISPR-edited hiPSCs derived beta like cell section) to determine *SLC30A8*  
525 knockdown and expression of the  $K_{ATP}$  channel genes (*ABCC8* Hs01093752\_m1 and *KCNJ11*  
526 Hs00265026\_s1; ThermoFisher Scientific). In Helsinki, EndoC- $\beta$ H1 cells were transfected with  
527 20nM siRNA and Scramble control. Following 96h of siRNA transfection, cells were incubated  
528 overnight in 1 mM glucose containing EndoC- $\beta$ H1 culture medium. One hour prior to glucose  
529 stimulation assay, the media was replaced by  $\beta$ KREBS (Univercell Biosolution S.A.S., France)  
530 without glucose. Cells were stimulated with 16.7 mM glucose and 50 mM KCl (Sigma-Aldrich) in  
531  $\beta$ KREBS for 30 min at 37°C in a CO<sub>2</sub> incubator. The cells were then washed and lysed with TETG  
532 (Tris pH8, Trito X-100, Glycerol, NaCl and EGTA) solution (Univercell Biosolution S.A.S.,  
533 France) for the measurement of total insulin content. Secreted and intracellular insulin were  
534 measured using a commercial human insulin Elisa kit (Mercodia AB, Uppsala, Sweden) as per  
535 manufacturer's instructions (Helsinki).

536 ***Electrophysiological measurements in EndoC- $\beta$ H1 cells (Oxford):*** *SLC30A8* was knocked down  
537 in EndoC- $\beta$ H1 as above.  $K^{+}_{ATP}$  channel conductance was measured in a perforated patch whole cell  
538 configuration, and patch-clamped using an EPC 10 amplifier and HEKA pulse software. KREBS  
539 extracellular solution was perfused in at 32°C and contained: 138 mM NaCl, 3.6 mM KCl, 0.5 mM  
540 MgSO<sub>4</sub>, 10 mM HEPES, 0.5 mM NaH<sub>2</sub>PO<sub>4</sub>, 5 mM NaHCO<sub>3</sub>, 1.5 mM CaCl<sub>2</sub>, 1 mM glucose and 100  
541  $\mu$ M Diazoxide (Sigma-Aldrich #D9035). The perforation of the membrane was achieved using an  
542 intra-pipette solution containing: 0.24 mg/mL amphotericin B, 128 mM K-gluconate (Sigma  
543 #Y0000005 and G4500 respectively), 10 mM KCl, 10 mM NaCl, 1 mM MgCl<sub>2</sub>, 10 mM HEPES,  
544 pH 7.35 (KOH). Conductance data are normalised to cell size and presented as pS.pF<sup>-1</sup>. Expression

545 of *ABCC8*, *KCNJ11*, *B2M*, and *TBP* were measured via qPCR as above (*SLC30A8* gene expression  
546 in CRISPR-edited hiPSCs derived beta like cell section).

547 ***Insulin and Proinsulin secretion and content (Helsinki):*** For the measurement of secreted insulin  
548 or proinsulin in the supernatant, 96h post-transfected cells were washed twice with 1X PBS and  
549 incubated with fresh EndoC-βH1 culture medium for next 24h. Secreted and intracellular insulin  
550 and proinsulin were measured using a commercial human insulin Elisa and human proinsulin Elisa  
551 kit from Mercodia (Mercodia AB, Uppsala, Sweden). Total cellular protein content was also  
552 determined with the BCA protein assay kit (Thermo Scientific, Pierce). Proinsulin to insulin ratio  
553 was calculated by dividing the respective values measured from the supernatant and the cells  
554 (pmol/L).

555 ***Immunoblotting (Helsinki):*** Total cellular protein was prepared with Laemmli buffer and resolved  
556 using Any kD Mini-Protean-TGX gel (Bio-Rad). Immunoblot analysis was performed by overnight  
557 incubation of with primary antibodies against ZNT8 (Abcam; #ab136990; 1:500), PC1/3 (Cell  
558 Signaling; #11914; 1:1000), CPE (BD Bioscience; #610758; 1:1000), Phospho-AKT-Ser473 (Cell  
559 Signaling; #4060; 1:1000), AKT (Santa-Cruz; #SC-8312; 1:500). The membranes were further  
560 incubated with species-specific HRP-linked secondary antibodies (1:5000) and visualization was  
561 performed following ECL exposure with ChemiDoc XRS+ system and Image Lab Software (Bio-  
562 Rad). A loading control of either alpha-Tubulin (Sigma; T5168; 1:5000) or beta-actin (Sigma;  
563 A5441; 1:5000) was performed on the same blot for all western blot data. Densitometric analysis of  
564 bands from image were calculated using Image J (Media Cybernetics) software and intensities  
565 compared as ZNT8, PC1/3, phosphor-AKT-Ser473 to tubulin; CPE to beta-actin.

566 ***Cell viability assay, MTT (Helsinki):*** EndoC-βH1 cells were transfected with either siScramble or  
567 siSLC30A8 for 96h. The viability of cells after 24 h of tunicamycin (10 µg/ml) treatment was  
568 determined using Vybrant MTT Cell proliferation kit (ThermoFisher Scientific; #M6494), the

569 standard MTT [3-(4,5-dimethylthiazol-2-yl)-2,5-diphenyltetrazolium bromide] assay. All the  
570 treatments were performed on cells with equal seeding density ( $5 \times 10^4$  cells/well) in 96 wells plate.  
571 The purple formazan crystals generated after 2 h incubation with MTT buffer were dissolved in  
572 DMSO, and the absorbance was recorded on a microplate reader at a wavelength of 540nm.

573 **RNA (mRNAs) sequencing of EndoC- $\beta$ H1 cells:** For RNA sequencing post 96h siScramble  
574 (n=3) or siSLC30A8 (n=3) transfected EndoC- $\beta$ H1 cells were used and the total RNA was  
575 extracted with Macherey-Nagel RNA isolation kit as per manufacturer's instruction. RNA  
576 sequencing was performed using Illumina TruSeq-mRNA library on NextSeq 500 system (Illumina)  
577 with an average of >15 million paired-end reads (2  $\times$  75 base pairs). RNA sequencing reads were  
578 aligned to hg38 using STAR (Spliced Transcripts Alignment to Reference)<sup>51</sup>, genome annotations  
579 were obtained from the GENCODE (Encyclopedia of Genes and Gene Variants) v22<sup>52</sup> program, and  
580 reads counting were done using featureCounts<sup>53</sup>. Further downstream analysis was performed using  
581 edgR<sup>54</sup> software package, low expressed (<1 average count per million) genes were removed, read  
582 counts were normalized using TMM<sup>55</sup> (trimmed mean of M-values), differential expression analysis  
583 was performed using method similar to Fisher's Exact Test and corrected for multiple testing using  
584 FDR (1%).

585 **Data Analyses:** Data are reported as mean (SEM). Statistical analyses were performed using Prism  
586 6.0 (GraphPad Software). All parameters were analyzed using Mann-Whitney test or Unpaired  
587 Student's t-test as indicated.

## 588 **Mouse Model**

589 **Animals:** All procedures were conducted in compliance with protocols approved by the Regeneron  
590 Pharmaceuticals Institutional Animal Care and Use Committee. The *Slc30a8*<sup>Tgp.Arg138\*</sup> mouse line is  
591 made in pure C57Bl/6 background by changing nucleotide 409 from T into C in exon 3, which  
592 changes the arginine into a stop codon<sup>11</sup>. The mutated allele has a self-deleting neomycin selection

593 cassette flanked by loxP sites inserted at intron 3, deleting 29 bp of endogenous intron 3 sequence.  
594 Mice were housed (up to five mice per cage) in a controlled environment (12-h light/dark cycle,  
595 22C, 60–70% humidity) and fed *ad libitum* with either chow (Purina Laboratory 23 Rodent Diet  
596 5001, LabDiet) or high-fat diet (Research Diets, D12492; 60% fat by calories) starting at age of 20  
597 weeks. All data shown are compared to their respective WT littermates.

598 **Glucose Tolerance Test:** Mice were fasted overnight (16 hr) followed by oral gavage of glucose  
599 (Sigma) at 2 g/kg body weight. Blood samples were obtained from the tail vein at the indicated  
600 times and glucose levels were measured using the AlphaTrak2 glucometer (Abbott). Submandibular  
601 bleeds for insulin were done at 0, 15, and 30 min post-injection.

602 **Hormone measurements:** Submandibular bleeds of either overnight fasted or fed animals were  
603 done in the morning. Plasma insulin or proinsulin was analyzed with the mouse insulin/proinsulin  
604 EIA (Mercodia AB, Uppsala, Sweden), and C-peptide with the mouse C-peptide EIA (ALPCO). All  
605 EIAs were performed according to the manufacturer's instructions.

606 **Data Analyses for mouse studies:** Data are reported as mean (SEM). Statistical analyses were  
607 performed using Prism 6.0 (GraphPad Software). All parameters were analyzed by two-way  
608 ANOVA or Unpaired Student's t-test as indicated.

#### 609 **Expression of p.Arg138\* mutation in INS1E**

610 INS-1E cells<sup>56</sup> were used for transient transfection of pcDNA3.1(+-)p.Arg138\* construct fused to  
611 fluorescent m-Cherry at C-terminus using transfection reagent Viromer according to the  
612 manufacturer's instructions. After transfections cells were collected at 24, 48, 72 and 96 hours and  
613 analysed by western blot analysis using mCherry (600-401-P16, Rockland) antibody. Untransfected  
614 cells were used as control and tubulin as a loading control. Two days after transient transfections  
615 with either p.Arg138\*-mCherry (INS1E), p.Arg138\*-HA or p.Arg138\*-Myc-His construct  
616 (INS1E), cells were washed with PBS twice and fixed using 4% paraformaldehyde for 15 min at

617 room temperature. Cells were permeabilized with 0.2 % Triton X-100 in phosphate-buffered saline  
618 (PBS) for 10 mins and to prevent unspecific binding were further blocked for 1 h with 5% FBS in  
619 PBS. INS1E cells transfected with either p.Arg138\*-HA or p.Arg138\*-Myc-His construct were  
620 incubated with the primary antibody (HA antibody: MMS-101P, Biolegend; His antibody: D291-  
621 A48, MBL; insulin antibody: A0564, DAKO), overnight at 4°C. Secondary antibodies were  
622 conjugated to Alexa Fluor 488 (Molecular Probes). Cells transfected with mCherry construct were  
623 imaged after 48 and 96 hours (INS1E) in order to visualize subcellular localization at different time  
624 points.

625 **Measurements of cytosolic zinc in INS-1(832/13) cells**

626 ***Cell culture:*** INS-1 (823/13) cells were grown in RPMI 1640 medium (Sigma-Aldrich, UK)  
627 supplemented with 10% (v/v) foetal bovine serum (FBS), 2 mM L-glutamine, 0.05 mM 2-  
628 mercaptoethanol, 10 mM HEPES (Sigma-Aldrich), 1 mM sodium pyruvate (GIBCO, France), 2  
629 mM L-glutamine and antibiotics (100 µg/ml Streptomycin and 100 U/ml penicillin). Cells were  
630 maintained in 95% oxygen, 5% carbon dioxide at 37°C.

631 ***Co-transfection:*** Cells were seeded on sterile coverslips at 60% confluence and co-transfected  
632 using lipofectamine 2000 (Invitrogen, USA) according to the manufacturer's instructions, with  
633 either the empty construct (EV) or the rare-truncated variant (c-Myc tag, R138X) construct and the  
634 Förster Resonance Energy transfer sensors (FRET), eCALWY-4 vector (free cytosolic zinc  
635 measurements).

636 ***Protein extraction and Western (immuno-) blotting analysis:*** For protein extraction, RIPA buffer  
637 (1% Triton X-100, 1% sodium deoxycholate, 0.1% SDS, 0.15 mM NaCl, 0.01 M sodium Phosphate  
638 pH7.2) was used for lysis. Protein extracts were resolved in SDS-page (12% vol/vol acrylamide)  
639 and transferred to a polyvinylidene fluoride (PVDF) membrane, followed by blocking for 1 hour,  
640 immunoblotting with either c-Myc anti-mouse SLC30A8 (1:400) and the secondary anti-mouse

641 antibody (1:10000, Abcam), and then the mouse monoclonal anti-tubulin (1:10000) and secondary  
642 anti-mouse for tubulin (1:5000). Chemiluminescence detection reagent (GE Healthcare) was used  
643 before exposing to hyperfilms.

644 **Immunocytochemistry:** Cells were fixed in 4% (v/v) Phosphate-buffered saline/Paraformaldehyde  
645 (PFA). Cells were permeabilized in 0.5% (w/v) PBS/TritonX-100 and further saturated with  
646 PBS/BSA 0.1%. Cells were then incubated for 1 hour with the primary antibody, anti-c-Myc mouse  
647 antibody (1:200) followed by the secondary Alexa Fluor® 568 nm anti-mouse IgG (H+L, 1:1000  
648 Life Technologies, USA). Coverslips were mounted with mounting medium containing DAPI  
649 (Vectashield, USA) on microscope slides (ThermoScientific). Imaging was performed on a Nikon  
650 Eclipse Ti microscope equipped with a 63x/1.4NA objective, spinning disk (CAIRN, UK) using a  
651 405, 488 and 561 nm laser lines, and images were acquired with an ORCA-Flash 4.0 camera  
652 (Hamamatsu) Metamorph software (Molecular Device) was used for data capture.

653 **Cytosolic free Zn<sup>2+</sup> measurements:** Acquisitions were performed 24 hours after transfection using  
654 an Olympus IX-70 wide-field microscope with a 40x/1.35NA oil immersion objective and a zyla  
655 sCMOS camera (Andor Technology, Belfast, UK) controlled by Micromanager software. Excitation  
656 was provided at 433 nm using a monochromator (Polychrome IV, Till Photonics, Munich,  
657 Germany). Emitted light was split and filtered with a Dual-View beam splitter (Photometrics,  
658 Tucson, Az, USA) equipped with a 505dcxn dichroic mirror and two emission filters (Chroma  
659 Technology, Bellows Falls, VT, USA - D470/24 for cerulean and D535/30 for citrine). Cells were  
660 perfused for 4 minutes with KREBS buffer (140 mM NaCl, 3.6 mM KCl, 0.5 mM NaH<sub>2</sub>PO<sub>4</sub>, 0.2  
661 mM MgSO<sub>4</sub>, 1.5 mM CaCl<sub>2</sub>, 10 mM HEPES, 25 mM NaHCO<sub>3</sub>) without additives, next the buffer  
662 was changed to KREBS buffer containing 50 μM N,N,N',N'-tetrakis(2-  
663 pyridylmethyl)ethylenediamine (TPEN, Sigma) for 5 minutes, followed by perifusion with KREBS  
664 buffer containing 100 μM ZnCl<sub>2</sub> and 5 μM of the Zn<sup>2+</sup>-specific ionophore 2-mercaptopuridine N-  
665 oxide (Pyrithione, Sigma). Image analysis was performed using ImageJ software. Steady-state

666 fluorescence intensity ratio of acceptor over donor was measured, followed by the determination of  
667 the minimum and maximum ratios to calculate the free Zn<sup>2+</sup> concentration using the following  
668 formula:  $[Zn^{2+}] = Kd \cdot ( (R - R_{min}) / (R_{max} - R) )$ , in which Rmin is the ratio in the Zn<sup>2+</sup> depleted  
669 state, after addition of 50  $\mu$ M TPEN, and Rmax was obtained upon Zn<sup>2+</sup> saturation with 100  $\mu$ M  
670 ZnCl<sub>2</sub> in the presence of 5  $\mu$ M pyrithione.

671 **Human Pancreatic islets**

672 Experiments on primary human pancreatic islets were independently performed in two places 1)  
673 Oxford and 2) Lund university diabetes center (LUDC)

674 ***Human pancreatic islets from Oxford:*** Human pancreatic islets were isolated from deceased  
675 donors under ethical approval obtained from the human research ethics committees in Oxford  
676 (REC: 09/H0605/2, NRES committee South Central-Oxford B). All donors gave informed research  
677 consent as part of the national organ donation program. Islets were obtained from the Diabetes  
678 Research & Wellness Foundation Human Islet Isolation Facility, OCDEM, University of Oxford.  
679 All methods and protocols using human pancreatic islets were performed in accordance with the  
680 relevant guidelines and regulations in the UK (Human Tissue Authority, HTA). Expression data for  
681 SLC30A8 estimated by RNA sequencing as described previously<sup>57</sup>. For *in vitro* insulin secretion,  
682 islets were pre-incubated in Krebs-Ringer buffer (KRB) containing 2 mg/mL BSA and 1 mM  
683 glucose for 1 hour at 37°C, followed by 1-hour stimulation in KRB supplemented with 6mM  
684 glucose. Insulin content of the supernatant was determined by radioimmunoassay (Millipore UK  
685 Ltd, Livingstone, UK) as described previously<sup>58</sup>.

686 ***Human pancreatic islets from LUDC:*** Human pancreatic islets were obtained from the Human  
687 Tissue Laboratory (Lund University, [www.exodiab.se/home](http://www.exodiab.se/home)) in collaboration with The Nordic  
688 Network for Clinical Islet Transplantation Program ([www.nordicislets.org](http://www.nordicislets.org))<sup>59,60</sup>. All the islet donors  
689 provided their consent for donation of organs for medical research and the procedures were

690 approved by the ethics committee at Lund University (Malmö, Sweden, permit number 2011263).  
691 Islet preparation for cadaver donors, their purity check and counting procedure have been described  
692 previously<sup>61</sup>. Static *in vitro* insulin secretion assay from 91 islets (non-diabetic individuals) was  
693 performed as described previously<sup>61,62</sup>. Briefly, six batches of 12 islets per donor were incubated for  
694 1 hour at 37°C in Krebs Ringer bicarbonate (KRB) buffer in presence of 1 mM or 16.7 mM  
695 glucose, as well as 1 mM or 16.7 mM glucose together with 70 mM KCl. Insulin concentrations in  
696 the extracts was measured using a radioimmunoassay kit (Euro-Diagnostica, Malmö, Sweden). The  
697 Association of p.Trp325Arg genotype with expression of *SLC30A8* and other genes involved in  
698 insulin production and processing<sup>22</sup> was performed using RNA sequencing from islets of 140 non-  
699 diabetic individuals as described previously<sup>59,60</sup>. Briefly, RNA sequencing of islets was done using  
700 a HiSeq 2000 system (Illumina) for an average depth of 32.4 million paired-end reads (2 × 100 base  
701 pairs)<sup>59,60</sup>. RNA sequencing reads were aligned to hg19 using STAR (Spliced Transcripts  
702 Alignment to Reference)<sup>51</sup>. Genome annotations were obtained from the GENCODE (Encyclopedia  
703 of Genes and Gene Variants) v20<sup>52</sup> program and read counting was done using featureCounts<sup>53</sup>.  
704 Read counts were normalized to total reads (counts per million) and additionally across-samples  
705 normalization was done using TMM method<sup>55</sup>. Association analysis (so called eQTL) was  
706 performed on inverse normalized expression values using linear regression adjusted for age, sex and  
707 islets purity.

## 708 **Statistics**

709 Detail information regarding statistical tests used for each sub-study has been provided in their  
710 respective method section or with figure legends.

## 711 **Data availability**

712 The data that support the findings of this study are available from the corresponding author on  
713 reasonable request. Individual level data for the human study can only be obtained via the Biobank  
714 of The Institute of Health and Welfare in Finland.

715  
716  
717

718 **References**

1. Chabosseau, P., & Rutter, G.A. Zinc and diabetes. *Arch Biochem Biophys* **611**, 79-85 (2016).
2. Chimienti, F., Devergnas, S., Favier, A., & Seve, M. Identification and cloning of a beta-cell-specific zinc transporter, ZnT-8, localized into insulin secretory granules. *Diabetes* **53**, 2330-7 (2004).
3. Flannick, J. et al. Loss-of-function mutations in SLC30A8 protect against type 2 diabetes. *Nat Genet* **46**, 357-63 (2014).
4. Flannick, J. et al. Genetic discovery and translational decision support from exome sequencing of 20,791 type 2 diabetes cases and 24,440 controls from five ancestries *bioRxiv* (2018).
5. Parsons, D.S., Hogstrand, C., & Maret, W. The C-terminal cytosolic domain of the human zinc transporter ZnT8 and its diabetes risk variant. *FEBS J.* **285**, 1237-1250 (2018).
6. Sladek, R. et al. A genome-wide association study identifies novel risk loci for type 2 diabetes. *Nature* **445**, 881-5 (2007).
7. Lemaire, K. et al. Insulin crystallization depends on zinc transporter ZnT8 expression, but is not required for normal glucose homeostasis in mice. *Proc Natl Acad Sci U S A* **106**, 14872-7 (2009).
8. Pound, L.D. et al. Deletion of the mouse Slc30a8 gene encoding zinc transporter-8 results in impaired insulin secretion. *Biochem J* **421**, 371-6 (2009).
9. Wijesekara, N. et al. Beta cell-specific Znt8 deletion in mice causes marked defects in insulin processing, crystallisation and secretion. *Diabetologia* **53**, 1656-68 (2010).
10. Mitchell, R.K. et al. Molecular Genetic Regulation of Slc30a8/ZnT8 Reveals a Positive Association with Glucose Tolerance. *Mol Endocrinol.* **30**, 77-91 (2016).
11. Kleiner, S. et al. Mice harboring the human SLC30A8 R138X loss-of-function mutation have increased insulin secretory capacity. *Proc Natl Acad Sci* **115**(32), E7642-E7649 (2018).
12. Groop, L. et al. Metabolic consequences of a family history of NIDDM (the Botnia study): evidence for sex-specific parental effects. *Diabetes* **45**, 1585-93 (1996).
13. Tamaki, M. et al. The diabetes-susceptible gene SLC30A8/ZnT8 regulates hepatic insulin clearance. *J Clin Invest* **123**, 4513-24 (2013).
14. Rezania, A. et al. Reversal of diabetes with insulin-producing cells derived in vitro from human pluripotent stem cells. *Nat Biotechnol* **32**, 1121-33 (2014).
15. Miyaoka, Y., Chan, A.H., & Conklin, B.R. Using Digital Polymerase Chain Reaction to Detect Single-Nucleotide Substitutions Induced by Genome Editing. *Cold Spring Harb Protoc* (2016).
16. Scharfmann, R. et al. Development of a conditionally immortalized human pancreatic  $\beta$  cell line. *J Clin Invest* **124**, 2087-98 (2014).
17. Hastoy, B. et al. Electrophysiological properties of human  $\beta$ -cell lines EndoC- $\beta$ H1 and - $\beta$ H2 conform with human  $\beta$ -cells. *BioRxiv* (2017).
18. Braun, M. et al. Voltage-gated ion channels in human pancreatic beta-cells: electrophysiological characterization and role in insulin secretion. *Diabetes* **57**, 1618-28 (2008).
19. Srinivasan, S., Bernal-Mizrachi, E., Ohsugi, M., & Permutt, M.A. Glucose promotes pancreatic islet beta-cell survival through a PI 3-kinase/Akt-signaling pathway. *Am J Physiol Endocrinol Metab* **283**, E784-93 (2002).
20. Nicolson, T.J. et al. Insulin storage and glucose homeostasis in mice null for the granule zinc transporter ZnT8 and studies of the type 2 diabetes-associated variants. *Diabetes* **58**, 2070-83 (2009).
21. Vinkenborg, J.L. et al. Genetically encoded FRET sensors to monitor intracellular Zn<sup>2+</sup> homeostasis. *Nat Methods* **6**, 737-40 (2009).
22. Zhou, Y. et al. TCF7L2 is a master regulator of insulin production and processing. *Hum Mol Genet* **23**, 6419-31 (2014).
23. Kirchhoff, K. et al. Polymorphisms in the TCF7L2, CDKAL1 and SLC30A8 genes are associated with impaired proinsulin conversion. *Diabetologia* **51**, 597-601 (2008).

764 24. Jainandunsing, S. et al. A stable isotope method for in vivo assessment of human insulin synthesis and secretion. *Acta Diabetol* **53**, 935-944 (2016).

765 25. Ivanova, A. et al. Age-dependent labeling and imaging of insulin secretory granules. *Diabetes* **62**, 3687-96 (2013).

766 26. Gerber, P.A. et al. Hypoxia lowers SLC30A8/ZnT8 expression and free cytosolic Zn<sup>2+</sup> in pancreatic beta cells. *Diabetologia* **57**, 1635-44 (2014).

767 27. Wong, W.P. et al. Exploring the Association Between Demographics, SLC30A8 Genotype, and Human Islet Content of Zinc, Cadmium, Copper, Iron, Manganese and Nickel. *Sci Rep* **7** (1), 473 (2017).

768 28. Vergnano, A.M. et al. Zinc dynamics and action at excitatory synapses. *Neuron* **82**, 1101-14 (2014).

769 29. Prost, A.L., Bloc, A., Hussy, N., Derand, R., & Vivaudou, M. Zinc is both an intracellular and extracellular regulator of KATP channel function. *J Physiol* **559**, 157-67 (2004).

770 30. Ferrer, R., Soria, B., Dawson, C.M., Atwater, I., & Rojas, E. Effects of Zn<sup>2+</sup> on glucose-induced electrical activity and insulin release from mouse pancreatic islets. *Am J Physiol* **246**, C520-7 (1984).

771 31. Isomaa, B. et al., A family history of diabetes is associated with reduced physical fitness in the Prevalence, Prediction and Prevention of Diabetes (PPP)-Botnia study. *Diabetologia* **53**, 1709-13 (2010).

772 32. Ahlvist, E. et al. Novel subgroups of adult-onset diabetes and their association with outcomes: a data-driven cluster analysis of six variables. *Lancet Diabetes Endocrinol* **6**, 361-369 (2018).

773 33. Lindgren, O. et al. Incretin hormone and insulin responses to oral versus intravenous lipid administration in humans. *J Clin Endocrinol Metab* **96**, 2519-24 (2011).

774 34. Sluiter, W.J., Erkelens, D.W., Reitsma, W.D. & Doorenbos, H. Glucose tolerance and insulin release, a mathematical approach I. Assay of the beta-cell response after oral glucose loading. *Diabetes* **25**, 241-4 (1976).

775 35. Mohandas, C. et al. Ethnic differences in insulin secretory function between black African and white European men with early type 2 diabetes. *Diabetes Obes Metab* **20**, 1678-1687 (2018).

776 36. Navalesi, R., Pilo, A. & Ferrannini, E. Kinetic analysis of plasma insulin disappearance in nonketotic diabetic patients and in normal subjects. A tracer study with <sup>125</sup>I-insulin. *J Clin Invest* **61**, 197-208 (1978).

777 37. Delaneau, O., Zagury, J.F. & Marchini, J. Improved whole-chromosome phasing for disease and population genetic studies. *Nat Methods* **10** (1), 5-6 (2013).

778 38. Flannick, J. et al. Sequence data and association statistics from 12,940 type 2 diabetes cases and controls. *Sci Data* **4**, 170179 (2017).

779 39. Howie, B., Fuchsberger, C., Stephens, M., Marchini, J. & Abecasis G.R. Fast and accurate genotype imputation in genome-wide association studies through pre-phasing. *Nat Genet* **44**, 955-9 (2012)

780 40. Abecasis, G.R., Cardon, L.R., & Cookson, W.O. A general test of association for quantitative traits in nuclear families. *Am J Hum Genet* **66**, 279-92 (2000).

781 41. Yang, J., Lee, S.H., Goddard, M.E. & Visscher, P.M. GCTA: a tool for genome-wide complex trait analysis. *Am J Hum Genet* **88**, 76-82 (2011).

782 42. Bonetti, S. et al. Variants of GCKR affect both  $\beta$ -cell and kidney function in patients with newly diagnosed type 2 diabetes: the Verona newly diagnosed type 2 diabetes study 2. *Diabetes Care* **34**, 1205-10 (2011).

783 43. van de Bunt, M. et al. Insights into islet development and biology through characterization of a human iPSC-derived endocrine pancreas model. *Islets* **8**, 83-95 (2016).

784 44. Cong, L. et al. Multiplex genome engineering using CRISPR/Cas systems. *Science* **339**, 819-23 (2013).

785 45. Krentz, N.A.J. et al. Phosphorylation of NEUROG3 Links Endocrine Differentiation to the Cell Cycle in Pancreatic Progenitors. *Dev Cell* **41**, 129-142.e6 (2017).

786 46. Perez-Alcantara, M. et al. Patterns of differential gene expression in a cellular model of human islet development, and relationship to type 2 diabetes predisposition. *Diabetologia* **61**, 1614-1622 (2018).

787 47. Harries, L.W., Hattersley, A.T. & Ellard S. Messenger RNA transcripts of the hepatocyte nuclear factor-1alpha gene containing premature termination codons are subject to nonsense-mediated decay. *Diabetes* **53**, 500-4 (2004).

788 48. Ravassard, P. et al. A genetically engineered human pancreatic  $\beta$  cell line exhibiting glucose-inducible insulin secretion. *J Clin Invest* **121**, 3589-97 (2011).

789 49. Chandra, V. et al. RFX6 regulates insulin secretion by modulating Ca<sup>2+</sup> homeostasis in human  $\beta$  cells. *Cell Rep* **9**, 2206-18 (2014).

790 50. Thomsen, S.K. et al. Systematic Functional Characterization of Candidate Causal Genes for Type 2 Diabetes Risk Variants. *Diabetes* **65**, 3805-3811 (2016).

791 51. Dobin, A. et al. STAR: ultrafast universal RNA-seq aligner. *Bioinformatics* **29**, 15-21 (2013).

792 52. Harrow, J. et al. GENCODE: the reference human genome annotation for The ENCODE Project. *Genome Res.* **22**, 1760-74 (2012).

793 53. Liao, Y., Smyth, G.K. & Shi, W. featureCounts: an efficient general purpose program for assigning sequence reads to genomic features. *Bioinformatics* **30**, 923-30 (2014).

794 54. Robinson, M.D., McCarthy, D.J. & Smyth G.K. “edgeR: a Bioconductor package for differential expression analysis of digital gene expression data.” *Bioinformatics*, **26**, 139-140 (2010).

824 55. Robinson, M.D. & Oshlack, A. A scaling normalization method for differential expression analysis of RNA-seq  
825 data. *Genome Biol.* **11**, R25 (2010).

826 56. Asfari, M. et al. Establishment of 2-mercaptoethanol-dependent differentiated insulin-secreting cell lines.  
827 *Endocrinology* **130**, 167-78 (1992).

828 57. van de Bunt, M. et al. Transcript Expression Data from Human Islets Links Regulatory Signals from Genome-  
829 Wide Association Studies for Type 2 Diabetes and Glycemic Traits to Their Downstream Effectors. *PLoS Genet.*  
830 **11**(12), e1005694 (2015).

831 58. Ramracheya, R. et al. Membrane potential-dependent inactivation of voltage-gated ion channels in alpha-cells  
832 inhibits glucagon secretion from human islets. *Diabetes* **59**, 2198-208 (2010).

833 59. Ottosson-Laakso, E. et al. Glucose-Induced Changes in Gene Expression in Human Pancreatic Islets: Causes or  
834 Consequences of Chronic Hyperglycemia. *Diabetes* **66**, 3013-3028 (2017).

835 60. Fadista, J. et al. Global genomic and transcriptomic analysis of human pancreatic islets reveals novel genes  
836 influencing glucose metabolism. *Proc Natl Acad Sci U S A* **111**, 13924-9 (2014).

837 61. Rosengren, A.H. et al. Overexpression of alpha2A-adrenergic receptors contributes to type 2 diabetes. *Science*.  
838 **327**, 217-20 (2010).

839 62. Taneera, J. et al. Identification of novel genes for glucose metabolism based upon expression pattern in human  
840 islets and effect on insulin secretion and glycemia. *Hum Mol Genet* **24**, 1945-55 (2015).

841 **URLs**

844 GCTA, <http://cnsgenomics.com/software/gcta>; SHAPEIT,  
845 [http://mathgen.stats.ox.ac.uk/genetics\\_software/shapeit/shapeit.html](http://mathgen.stats.ox.ac.uk/genetics_software/shapeit/shapeit.html), IMPUTE2,  
846 [http://mathgen.stats.ox.ac.uk/impute/impute\\_v2.html](http://mathgen.stats.ox.ac.uk/impute/impute_v2.html);

848 **Acknowledgements**

849 We thank the Botnia Study Group for recruiting and studying the participants, Jens Juul Holst for  
850 measuring GLP-1 concentrations, and Linda Boselli, PhD, for carrying out mathematical modelling  
851 of the OGTT studies. We thank Erqian Na for her help with the mouse immunohistochemistry and  
852 histology, and Catherine Green and the Chromosome Dynamics & Genome Engineering Cores at  
853 the Wellcome Centre for Human Genetics for support with karyotyping and genome editing (funded  
854 by the Wellcome Trust grant 203141). The Botnia and The PPP-Botnia studies (L.G., T.T.) have  
855 been financially supported by grants from Folkhälsan Research Foundation, the Sigrid Juselius  
856 Foundation, The Academy of Finland (grants no. 263401, 267882, 312063 to LG, 312072 to TT),  
857 Nordic Center of Excellence in Disease Genetics, EU (EXGENESIS, EUFP7-MOSAIC FP7-  
858 600914), Ollqvist Foundation, Swedish Cultural Foundation in Finland, Finnish Diabetes Research  
859 Foundation, Foundation for Life and Health in Finland, Signe and Ane Gyllenberg Foundation,  
860 Finnish Medical Society, Paavo Nurmi Foundation, Helsinki University Central Hospital Research  
861 Foundation, Perklén Foundation, Närpes Health Care Foundation and Ahokas Foundation, as well  
862 as by the Ministry of Education in Finland, Municipal Health Care Center and Hospital in Jakobstad  
863 and Health Care Centers in Vasa, Närpes and Korsholm. The work described in this paper has been  
864 supported with funding from collaborative agreements with Pfizer Inc., as well as with Regeneron  
865 Genetics Center LLC. J.L. was supported by Vinnova - Sweden's Innovation Agency (2015-  
866 01549), Swedish Diabetes Foundation, Albert Pahlsson Foundation, Hjelt Foundations, Crafoord  
867 Foundation, Royal Physiographic Society in Lund, Swedish Foundation for Strategic Research  
868 (IRC15-0067), Swedish Research council (2009-1039, Strategic research area Exodiab); E.A. by  
869 Crafoord Foundation, Pahlsson Foundation, Swedish Research Council (Dnr: 2017-02688).; O.H.  
870 by Lund University Diabetes Center, ALF, Crafoord foundation, Novo Nordisk foundation, Magnus  
871 Bergvall foundation, Pahlsson foundation, Diabetes Wellness and Swedish Diabetes Research  
872 Foundation; R.C.B. by Italian Ministry of University and Research (PRIN 2015373Z39\_004) and  
873 University of Parma Research Funds; G.R. by a Wellcome Trust Senior Investigator Award  
874 (WT098424AIA), MRC Programme grants (MR/R022259/1, MR/J0003042/1, MR/L020149/1) and  
875 Experimental Challenge Grant (DIVA, MR/L02036X/1), MRC (MR/N00275X/1), Diabetes UK  
876 (BDA/11/0004210, BDA/15/0005275, BDA 16/0005485) and Imperial Confidence in Concept  
877 (ICiC) grants, and a Royal Society Wolfson Research Merit Award. ALG is a Wellcome Trust

878 Senior Fellow in Basic Biomedical Science. M.I.M. and P.R. are Wellcome Senior  
879 Investigators. This work was funded in Oxford by the Wellcome Trust (095101 [ALG], 200837  
880 [A.L.G.], 098381 [M.I.M.], 106130 [A.L.G., M.I.M.], 203141 (A.L.G., B.D., M.I.M.], 203141  
881 [M.I.M.], 090531 [P.R.]), Medical Research Council (MR/L020149/1) [M.I.M., A.L.G., P.R.],  
882 European Union Horizon 2020 Programme (T2D Systems) [A.L.G.], and NIH (U01-DK105535;  
883 U01-DK085545) [M.I.M., A.L.G.]. The research was funded by the National Institute for Health  
884 Research (NIHR) Oxford Biomedical Research Centre (BRC) [A.L.G., M.I.M., P.R.]. The views  
885 expressed are those of the author(s) and not necessarily those of the NHS, the NIHR or the  
886 Department of Health.

887

### 888 **Author Contributions**

889 M.L., L.S., T.T. and L.G. conducted the human study; E.A., O.H., A.B. and J.F. analyzed the  
890 genotype data ; M.L., O.P.D., M.T., E.B., R.C.B, T.T. and L.G. analyzed the human data; B.H.,  
891 N.L.B., S.K.T., M.vD.B., V.C., O.P.D., T.O. and A.L.G. characterized the Human beta-cell model;  
892 N.L.B., N.A.J.K., F.A., B.C., D.M., P.K., B.D., M.I.M. and A.L.G. characterized the human IPS  
893 cell derived model; U.K., R.P., O.P.D., B.H., A.J.P., I.S., R.R., I.A., P.R., M.I.M. and A.L.G.  
894 characterized the human islets; S.K., D.G. and J.G. characterized the *Slc30a8* p.Arg138\* mice; D.J.,  
895 J.L., P.C., A.T., R.C., A-M.R., J.B. and G.R. characterized the rat insulinoma cell-line; M.I.M.,  
896 A.L.G., T.T. and L.G. supervised the project; O.P.D., M.L., B.H., S.K., N.K., P.R., A.L.G., T.T.,  
897 and L.G. wrote the manuscript; all authors revised the manuscript.

898

### 899

### 900 **Materials & Correspondence**

901 Correspondence and requests for materials should be addressed to L.G. (leif.groop@med.lu.se)  
902 or A.L.G(anna.gloyn@drl.ox.ac.uk)

903

### 904

### 905 **Competing interests**

906 L.G. has received research funding from Pfizer Inc, Regeneron Pharmaceuticals, Eli Lilly and Astra  
907 Zeneca. N.L.B. and M.vD.B are now employees of Novo Nordisk, although all experimental work  
908 was carried out under employment at the University of Oxford. ALG has received honoraria from  
909 Novo Nordisk. MIM serves on advisory panels for Pfizer, Novo Nordisk, Zoe Global; has received  
910 honoraria from Pfizer, Novo Nordisk and Eli Lilly; has stock options in Zoe Global; has received  
911 research funding from Abbvie, Astra Zeneca, Boehringer Ingelheim, Eli Lilly, Janssen, Merck,  
912 Novo Nordisk, Pfizer, Roche, Sanofi Aventis, Servier, Takeda.

913

914

915

916

917

918  
919  
920  
921  
922  
923  
924  
925  
926  
927  
928  
929  
930  
931  
932  
933  
934  
935  
936  
937  
938  
939  
940  
941  
942  
943  
944  
945  
946  
947

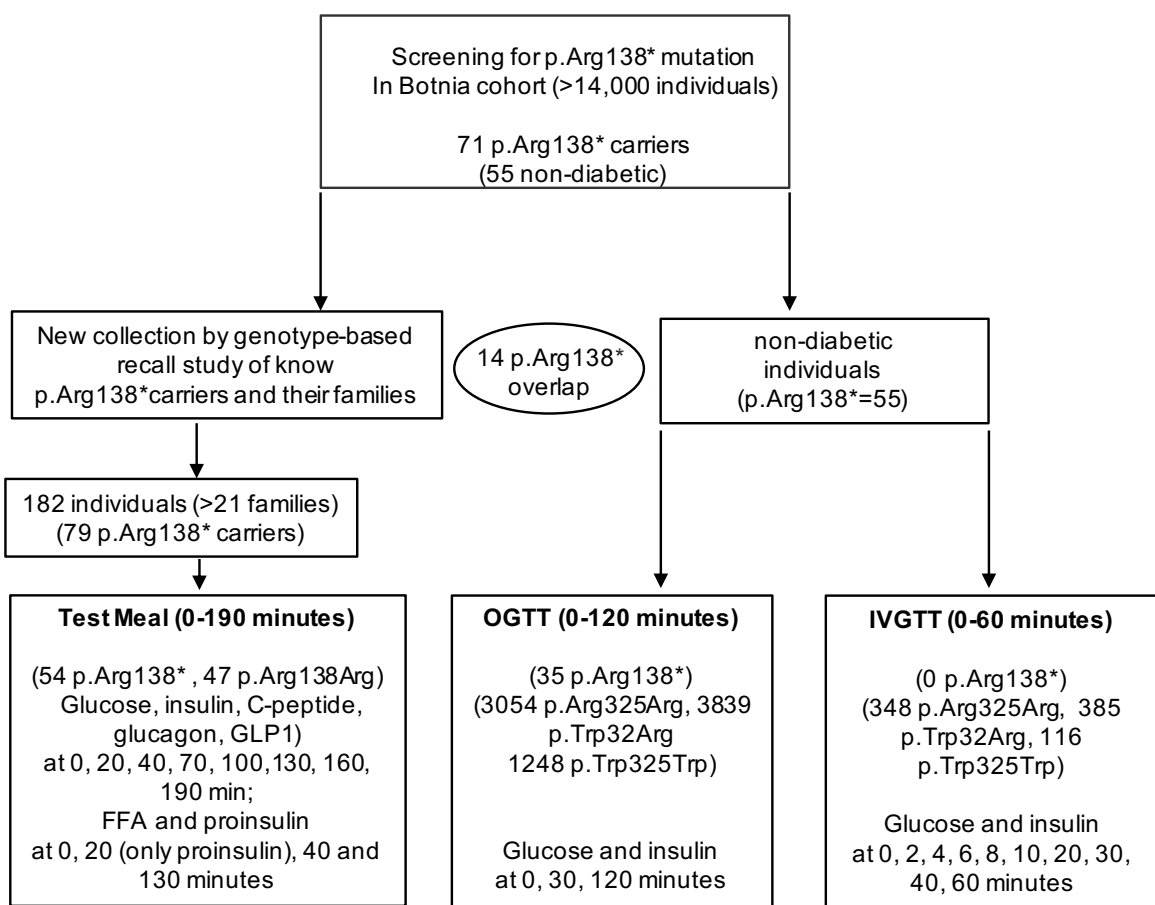
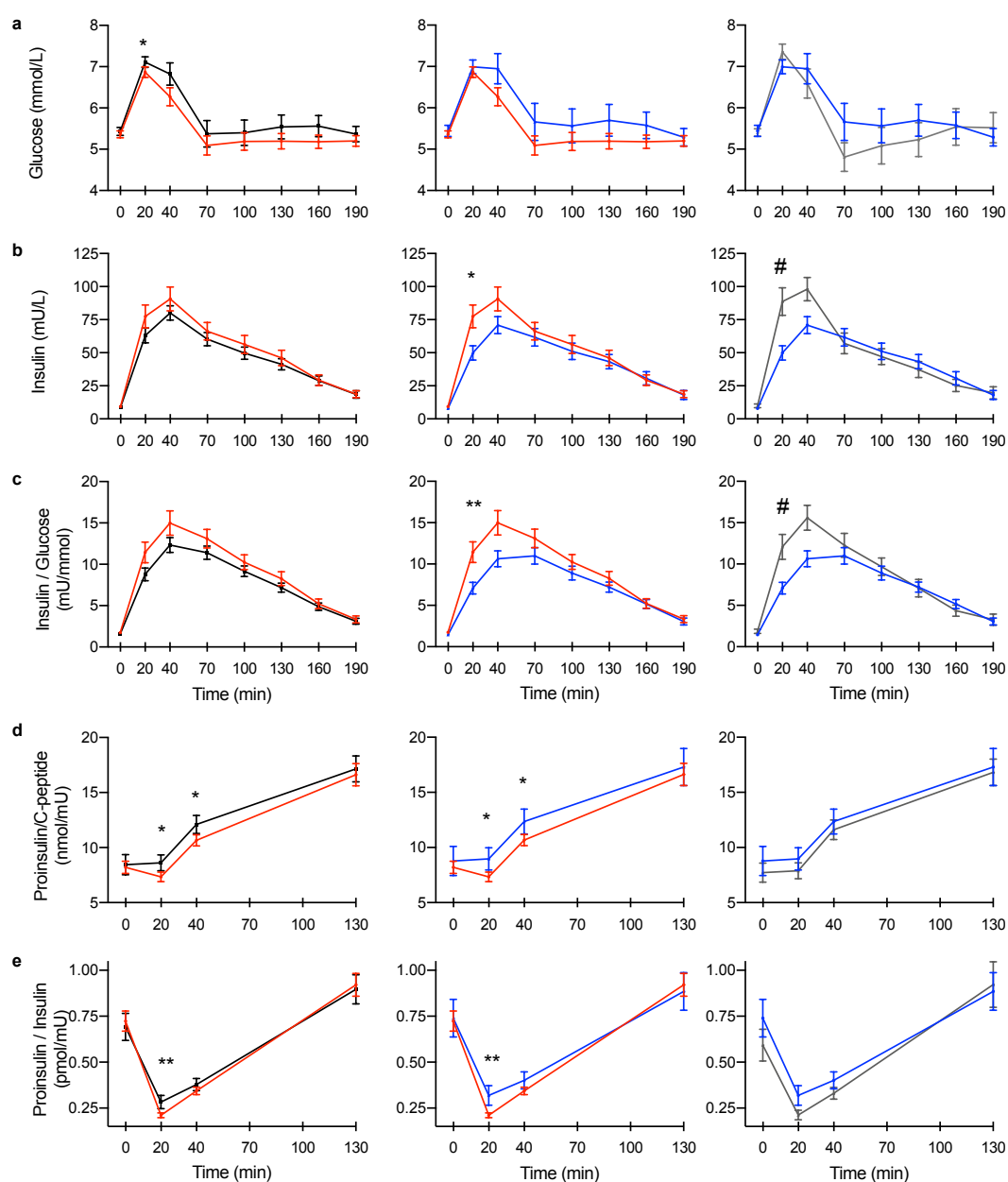


Fig. 1: A flow-chart of study design for human *in vivo* studies

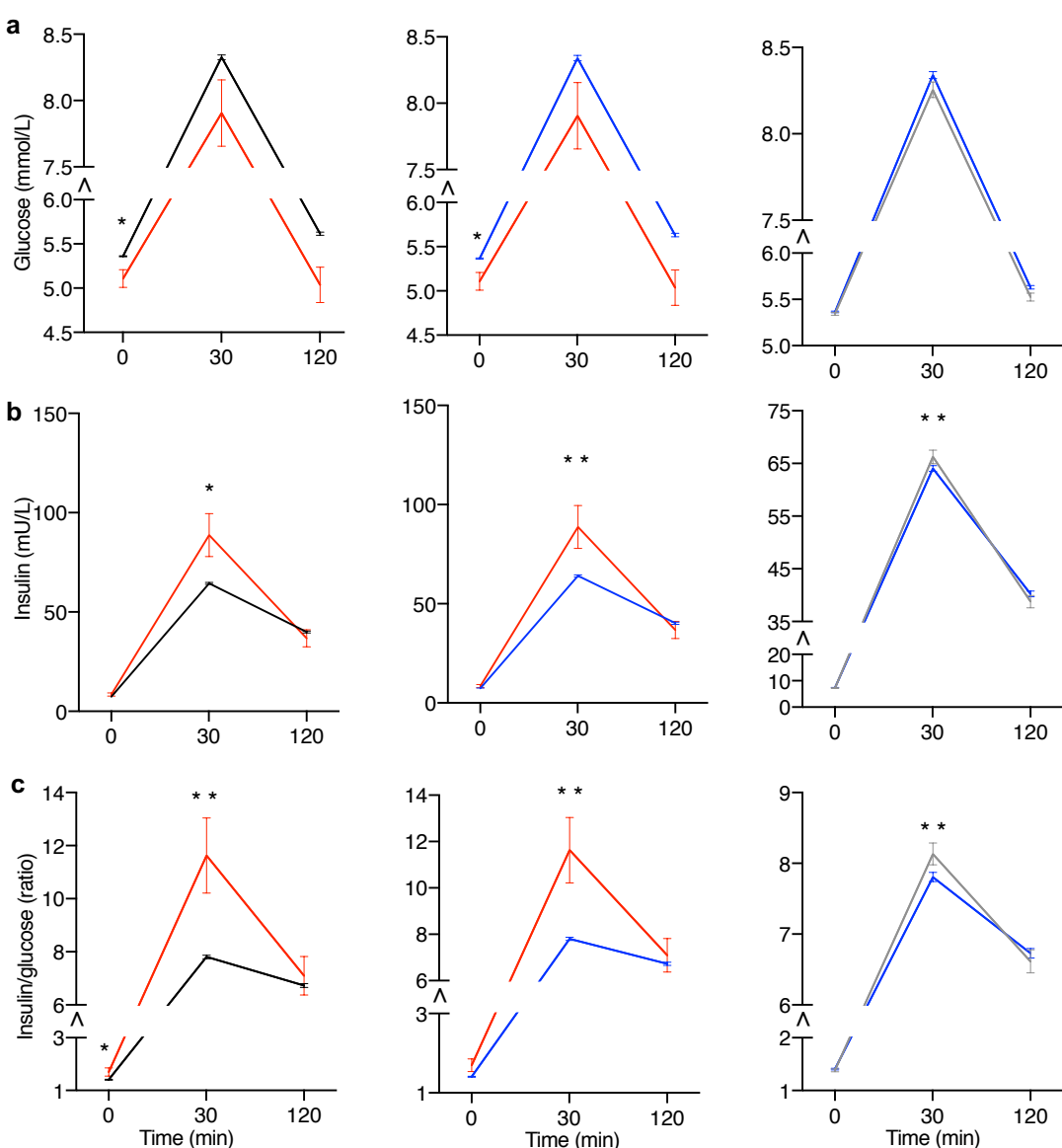
948



949 **Fig. 2: SLC30A8-p.Arg138\* enhances insulin secretion and proinsulin processing during test meal.**

950 Association of *SLC30A8* p.Arg138\* and p.Trp325Arg variants with **a**, plasma glucose **b**, serum insulin **c**,  
 951 insulin/glucose ratio **d**, proinsulin/C-peptide ratio and **e**, proinsulin/insulin ratio during test meal. *Left panel*: Carriers  
 952 (red, N=54) vs. non-carriers (black, N=47) of p.Arg138\*. *Middle panel*: Carriers of p.Arg138\* (red, N=54) vs  
 953 Arg138Arg having the common risk variant p.Arg325 (blue, N=31). *Right panel*: Carriers of p.Trp325Trp (grey, N=16)  
 954 vs. p.Arg325 (blue, N=31). Data are Mean  $\pm$  SEM. P-values were calculated by family-based association (\*) or linear  
 955 regression (#) (adjusted for age, sex, BMI and p.Trp325Arg variant status for the middle pane, Methods): \*/#, p < 0.05,  
 956 \*\*/##, p < 0.01.  
 957

958  
959  
960  
961  
962  
963  
964  
965  
966  
967  
968  
969  
970  
971  
972  
973  
974



983 **Fig. 3: *SLC30A8* p.Arg138\* and p.Trp325 enhance insulin secretion during OGTT.**  
984 Association of *SLC30A8* p.Arg138\* and p.Trp325Arg with **a**, plasma glucose **b**, serum insulin **c**, insulin/glucose ratio  
985 during an oral glucose tolerance test (OGTT). *Left panel*: Carriers (red, N=35) vs. non-carriers (black, N=7954-8141) of  
986 p.Arg138\*. *Middle panel*: Carriers of p.Arg138\* (red, N=35) vs. p.Arg138Arg having the common risk variant  
987 p.Arg325 (blue, N=6728-6893). *Right panel*: Carriers of p.Trp325Trp (grey N=1226-1248) vs. p.Arg325 (blue,  
988 N=6728-6893). Data are shown as Mean  $\pm$  SEM. P-values (mixed model, Methods) using additive effect: \* < 0.05, \*\* <  
989 0.01. Y-axis: note truncation ( $\wedge$ ) and different scale in the right panel.

990  
991  
992  
993  
994

995  
996  
997  
998  
999

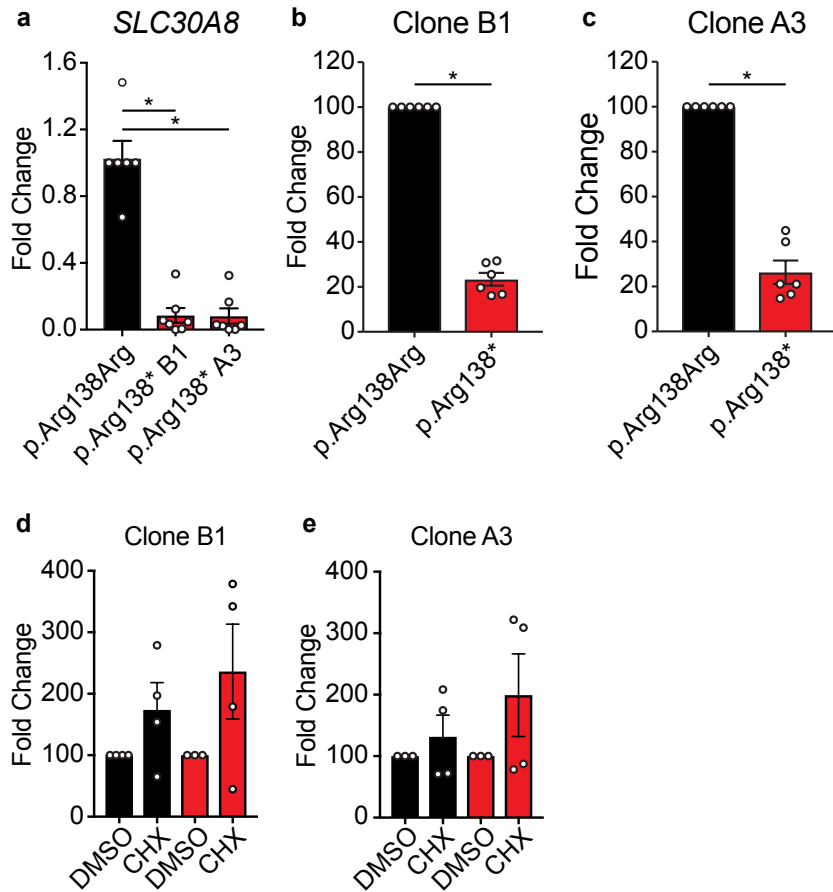
1000  
1001  
1002  
1003  
1004  
1005  
1006  
1007  
1008  
1009  
1010  
1011

1012  
1013

1014  
1015  
1016  
1017  
1018  
1019  
1020  
1021  
1022

1023 **Fig. 4: Beta like cells derived from *SLC30A8*-p.Arg138\* iPSCs display haploinsufficiency of *SLC30A8*.**

1024 **a**, *SLC30A8* expression in cells heterozygous for *SLC30A8*-p.Arg138\*. Data normalized to *TBP* gene are expressed as  
1025 fold change relative to p.Arg138Arg control (n=6-7 wells from two differentiations). Allele-specific expression (ASE)  
1026 of p.Arg138Arg (black bar) and p.Arg138\* (red bar) in **b**, clone B1 or **c**, clone A3 derived cells. Allele-specific  
1027 expression of p.Arg138Arg (black bar) and p.Arg138\* (red bar) in **d**, clone B1 and **e**, clone A3 derived cells treated  
1028 with DMSO (Dimethyl sulfoxide) or cycloheximide (CHX) for four hours. ASE data (Mean  $\pm$ SEM) were determined  
1029 by Digital Droplet PCR and presented as fold change relative to p.Arg138Arg transcript (**b**, **c**, n=6 wells from two  
1030 differentiations) or to DMSO control (**d**-**e**, n=3-4 wells from two differentiations). \* P<0.05 (Kruskal-Wallis test for  
1031 multiple comparisons or unequal variance t-test).  
1032



1033  
1034  
1035  
1036  
1037  
1038  
1039  
1040  
1041  
1042  
1043  
1044  
1045  
1046  
1047  
1048  
1049  
1050  
1051  
1052  
1053  
1054  
1055  
1056  
1057  
1058  
1059  
1060  
1061  
1062  
1063  
1064  
1065  
1066  
1067  
1068  
1069  
1070  
1071  
1072

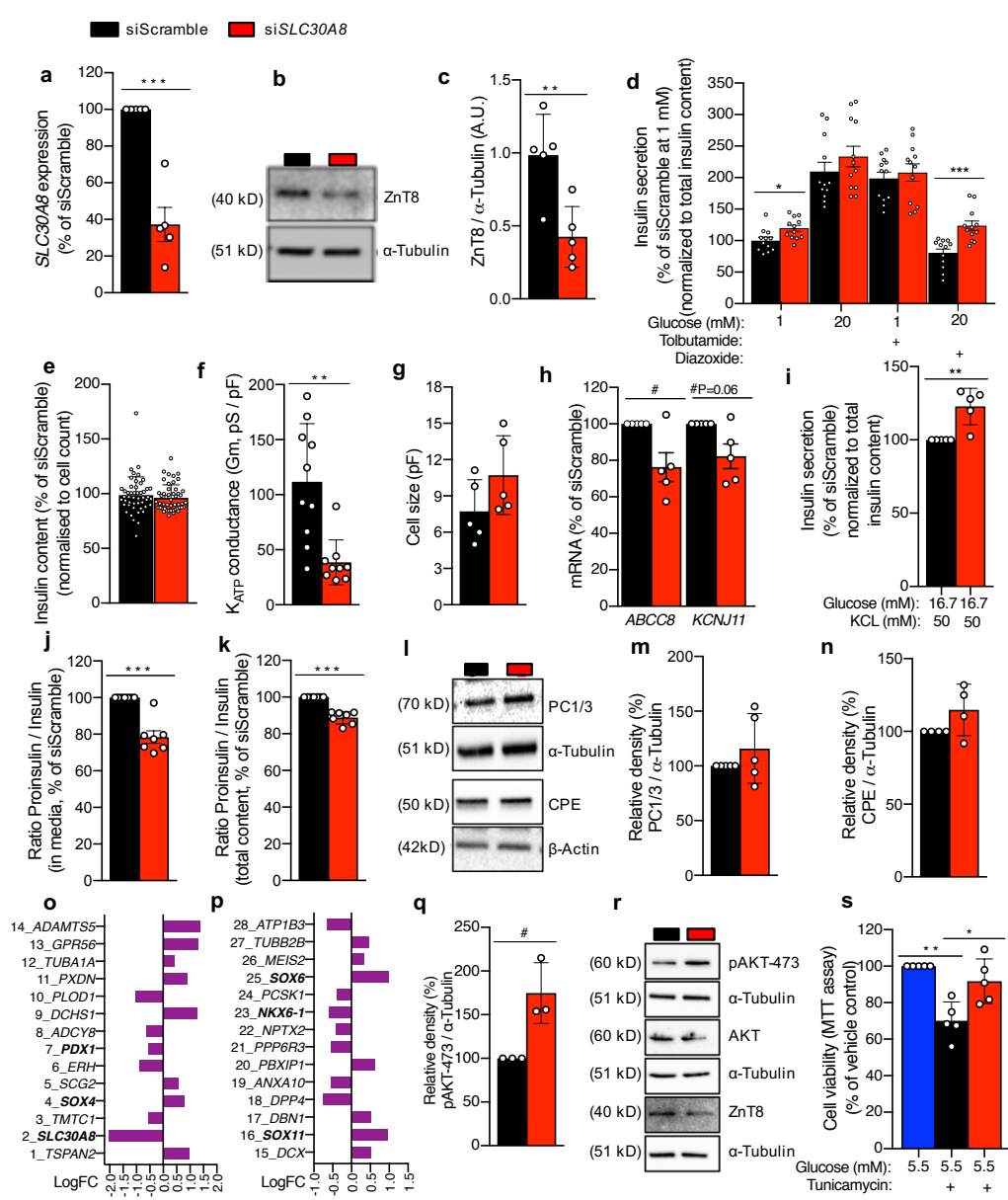
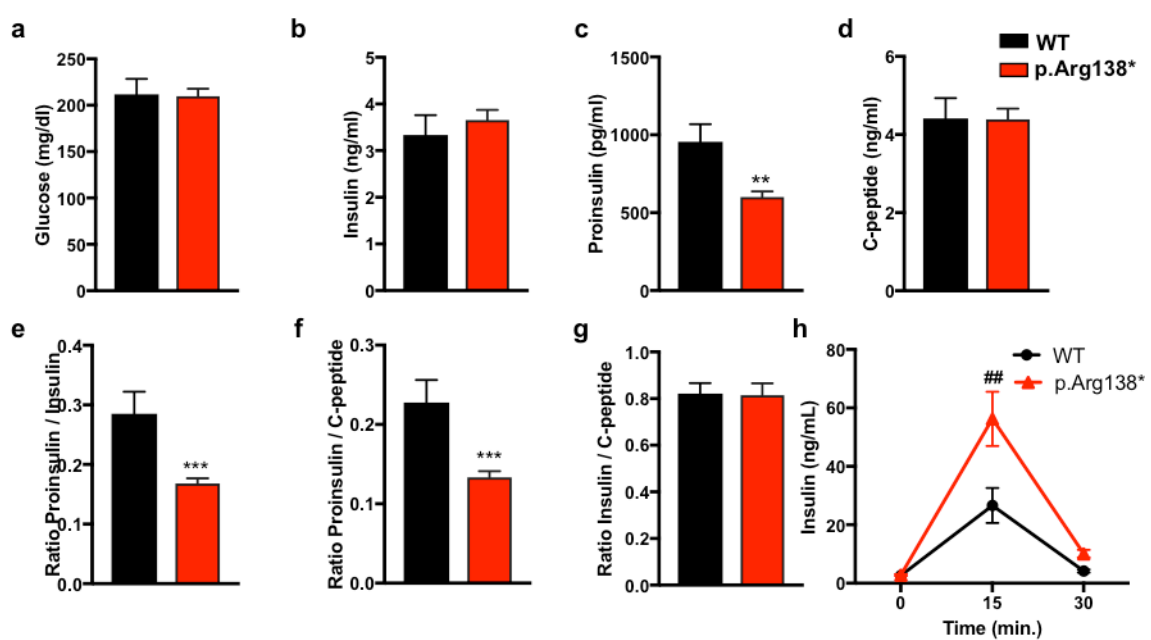


**Fig. 5: SLC30A8 knock down leads to enhanced insulin secretion, proinsulin processing and cell viability in the human pancreatic EndoC- $\beta$ h1 cells.**

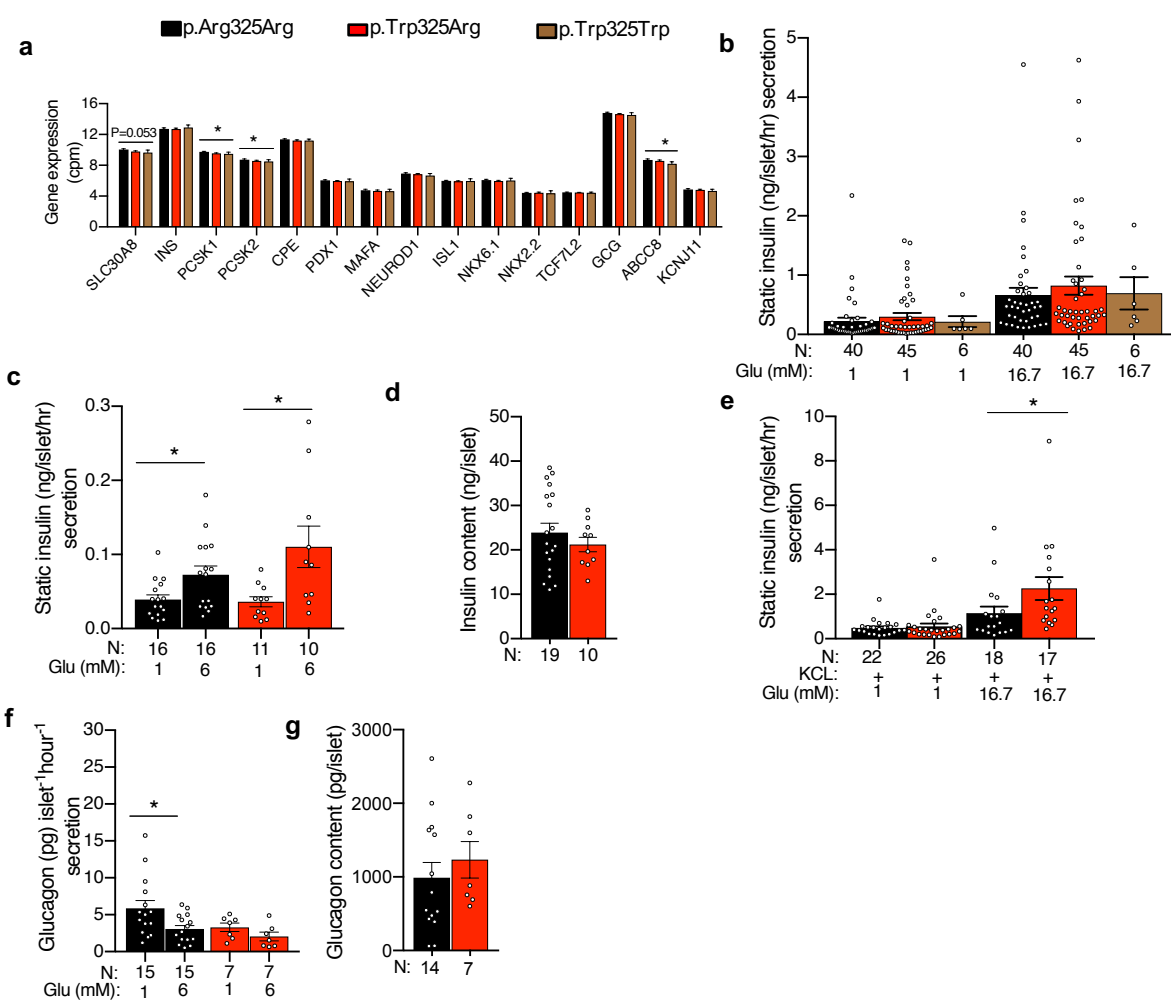
**a-c**, Characterization of SLC30A8 knock down (KD) at the (a) mRNA and protein level (b-immunoblot, c-densitometry). **d-i**, Effect of KD on (d) insulin secretion stimulated by glucose and K<sub>ATP</sub> channel regulators (as labelled), (e) insulin content, (f) K<sub>ATP</sub> channel conductance (Gm), (g) cell size, (h) expression of K<sub>ATP</sub> channel subunits, (i) insulin secretion stimulated by KCl and high glucose. **j-n**, Effect of KD on proinsulin processing estimated by (j-k) proinsulin/insulin ratio and proinsulin processing enzymes PC1/3 and CPE (l, immunoblot, m-n, densitometry). **o-p**, Effect of KD (n=3 vs. 3) on whole transcriptome (mRNAs) by next generation sequencing and depicting 28 top candidate genes ranked by increasing p values (1% FDR corrected, P≤0.0002). **q-s**, Effect of KD on basal (5.5 mM glucose) AKT phosphorylation (q, densitometry, r, immunoblot; phospho-AKT-Ser473, total AKT) and cell viability under ER stress (s, MTT assay, 10 µg/ml tunicamycin, DMSO as vehicle control). Data are shown as Mean ±SEM (N=3-10). P-values (\*Mann-Whitney test/#Unpaired t test): \*/# p≤0.05, \*\* p < 0.01, \*\*\* p < 0.001.



1091 **Fig. 6: Male p.Arg138\* mice on high-fat diet show enhanced insulin secretion and proinsulin processing.**

1092 Circulating **a**, glucose **b**, insulin **c**, proinsulin **d**, C-peptide **e**, proinsulin/insulin ratio **f**, proinsulin/C-peptide ratio and **g**,  
1093 insulin/C-peptide ratio in fasted WT and p.Arg138\* mice (n= 10 WT, 17 p.Arg138\*) after 20 weeks on HFD. **h**, Insulin  
1094 response to oral glucose (2g/kg) exposure (n=5 WT, 11 p.Arg138\*) after 30 weeks on HFD. p\*\*<0.01, p\*\*\*<0.005 using  
1095 Students T test; p##<0.01 using two-way Anova.

1099



1100

1101 **Fig. 7: SLC30A8- p.Trp325 leads to enhanced insulin secretion in human islets.**

1102 **a**, Effect of p.Trp325Arg genotype (p.Arg325Arg=66, p.Trp325Arg=63 and p.Trp325Trp=11) on expression of  
1103 SLC30A8 and other genes involved in insulin production, secretion and processing. **b**, Effect of p.Trp325Arg genotype  
1104 on static insulin secretion in presence of low and high glucose stimulatory conditions. **c-d**, Effect of p.Trp325Arg  
1105 genotype on static insulin secretion in (**c**) low stimulatory conditions and their (**d**) insulin contents. **e**, Effect of  
1106 p.Trp325Arg genotype on static insulin secretion in presence of low and high glucose and KCL. **f**, Static glucagon  
1107 response to glucose and **g**, glucagon content at basal glucose. Data are Mean  $\pm$  SEM; Glu- glucose. Analysis by linear  
1108 regression or Mann-Whitney test (Methods); \* p<0.05.

1109

1110

1111

1112